Remote Sensing and Sustainability Analysis of Sugarcane within the Everglades Agricultural Area

Remote Sensing and Sustainability Analysis of Sugarcane within the Everglades Agricultural Area

Brandon McBath

A Thesis in the Field of Sustainability

for the Degree of Master of Liberal Arts in Extension Studies

Harvard University

March 2023

Abstract

I evaluated the relationship of nitrogen runoff and the practice of burning sugarcane in Everglades Agricultural Area (EAA) in southern Florida. The soil in the EAA is composed of nitrogen rich peat, which is a few inches to many feet deep over a limestone base. Over time the peat begins to break down due to oxidation, drying, temperature (Qualls & Richardson, 2008), and burning. Prior to harvesting the sugarcane, the fields are burned to remove excess green vegetation, leaving behind sugarcane burn residue (BR). Sugarcane burning results in exposed soil, which allows for precipitation to erode the BR and decaying peat (Bordonal et al., 2018). Nutrient loss in BR is also statistically more sensitive to precipitation (Udeigwe et al., 2009). The nutrient loss, due to runoff and peat decomposition, results in a net loss of nitrogen in the sugarcane fields and nutrification in downgradient wetlands (SFWMD, 2020).

A research gap exists for assessing the correlation of sugarcane burning and nitrogen nutrification within the EAA and downstream wetlands. To address this knowledge gap, I tested the hypotheses that: 1a) there is a direct correlation between the sugarcane field burning within the EAA and increased nitrogen, with precipitation as a driving transport mechanism, within the downgradient water; 1b) regional differences exist between the scale of the burning each year and soil nutrient loss as measured through water quality observations; 2a) substantial environmental benefits can be realized by mitigating N impacts by altering sugarcane farming practices to reduce burning; and 2b) some of the alternative practices to burning are cost-effective.

To determine the relationship between the traditional sugarcane practice of pre-harvest burning and nitrogen levels in nearby wetlands, I first defined a study area within EAA that was hydraulically confined by major canals. I obtained precipitation and nitrogen levels from multiple Water Quality Stations (WQS) and satellite imagery for remote sensing analyses, specifically utilizing the normalized difference vegetation index (NDVI) to evaluate healthy sugarcane versus burned ground. I evaluated the data to determine statistical outlying data points, with nitrogen representing soil loss, precipitation as the erosional driving mechanism, and NDVI as the evaluation of the current ground cover. I was able to statistically correlate burned ground to the NDVI in the study area. The NDVI, precipitation, and nitrogen outlying values were indirectly correlated by graphing them as a twenty-year time-series and observing the seasonal trends. The results of the time-series analysis indicated an indirect correlation between the sugarcane burning and nitrogen levels and the results varied regionally.

To determine if sustainable change be made to the commercial sugarcane industry, I devised three cost-benefit analyses (CBA) of alternatives: replacing sugarcane harvesters with a more efficient model; processing the green trash and bagasse into biochar for resale; and planting cover crop, Sunn Hemp, during the fallow year to aid in soil stabilization, nutrient loss prevention, and pest control. The results of the CBA indicated all three are viable options. Options 2 and 3 indicated significant potential to improve the soil and as a result reduce the environmental impact due to soil loss. The conclusions of my research indicated multiple possible solutions to the environmental impact and soil loss to sugarcane farming while still remaining profitable, resulting in a prosperous sustainable symbiotic future for the sugarcane industry and the environment.

Frontispiece

Dedication

I dedicate my thesis to my family. Thank you to my wife in particular for helping motivate and keep me on track; you are amazing.

Acknowledgments

Thank you to Dr. Magaly Koch for all of the many, many hours of discussion we had throughout this thesis process. Your guidance made this possible. Thank you to Dr. Mark Leighton for all of your help and guidance at the beginning and end of this thesis process. You helped me focus my thoughts and build a clearer vision of what I wanted to research.

Table of Contents

List of Tables

List of Figures

Chapter I

Introduction

The Everglades is unique and important wetland that was on the brink of destruction in the 20th century due to development and nutrient pollution impacts, especially of nitrogen and phosphorous. Though extensive work has been done to repair the damage, the ecosystem is still precariously balanced with human civilization, specifically commercial agriculture and its practices. A portion of the Everglades was originally developed as agricultural land in the late 19th century. As technology improved, so did the expansion and breadth of land development in the Everglades. Expansion during the 20th century, due to the rapidly increasing demand for sugar, was the most pervasive, causing widespread harm to the various ecosystems by rerouting their natural surface water flow (Sandhu et al., 2016). Significant and costly efforts have been made, since major restoration efforts began in the 1970s, to improve hydrology to more closely resemble the original natural flow while still maintaining use of the EAA (Everglades Agricultural Area).

The commercial sugarcane industry began around 1920 in the counties around the south and southeast side of Lake Okeechobee (Heitmann, 1998). Florida produces 53.8% of total sugarcane within the United States (Schmitz & Zhang, 2019) and the Everglades Agricultural Area (EAA), which is approximately 700,000 acres (Daroub, Diaz, & Chen, 2018), comprises approximately 400,000 acres of the Florida production (Rott et al., 2018). In 1960, the United States embargo on Cuba resulted in a significant expansion of the sugarcane production in Florida, from approximately 50,000 acres to several hundred

thousand acres over the next several decades (Baucum & Rice, 2009). Demand for sugar has also increased significantly, thus resulting in increased production, increased environmental impact, and an increased economic status.

Nutrient runoff pollution from the EAA, significantly influenced and controlled by precipitation, and soil loss are problems of great importance and a focus for state agencies due to the now permanent presence of sugar cane agriculture. As with most commercial agriculture, fertilization is utilized to ensure healthy sugar cane crops mainly through the application of phosphorus (P) and potassium. The most prevalent nutrient monitored in the sugarcane fields is P (Corstanje et al., 2016; Lang, 2010). The amount of nitrogen (N) fertilization varies, and can be zero, based on the levels of N within the soil. Since the increase in commercial production of sugarcane in the1920s, the intensity of nutrient impact has steadily increased.

However, before a sugarcane field is harvested, the field is burned to remove the unwanted debris. The field burning is efficient in removing undesired material, but is associated with leaching N and significant nutrient loss. Peat also becomes more flammable as the sugarcane fields are relatively dry during harvest. Peat decay and subsequent soil and nutrient loss through erosion has been an on-going problem for the EAA for decades (UF IFAS, 2009). The burning exacerbates these effects.

A major water quality concern that has arisen is nutrient runoff and seepage into the adjacent wetlands as many of the native plants are adversely affected by the increased nutrient levels. Therefore most of the mitigation effort has been spent on the reduction of P loads in the water being moved out of the EAA (Daroub, 2011). Due to the naturally

occurring elevated N levels, less research and mitigation has been performed to assess the scale of N pollution and address its possible mitigation (SFWMD, 2019).

Research Significance and Objectives

To address the gap in the N research, and to lesser effect soil loss, my research examined the relationship of N runoff and the practice of burning sugarcane. I evaluated burn alternative scenarios for mitigating N and devised multiple cost-benefits analyses for these scenarios. The cost-benefit analyses could allow the sugar industry to improve their best practices, while staying profitable and sustainable, and reduce their impact on the Everglades.

My objectives were:

- To determine significance between specific climatic and soil environmental variables, precipitation (as a mechanism to N loss) and N, and the burned sugarcane fields that have an impact on the wetland nitrogen level, as determined by water quality analysis
- To determine if any region within my study area has a more measurable environmental impact effect from N pollution, due to an increased area of burning, i.e., regional spatial impacts
- To conduct economic cost-benefit analyses to compare various scenarios of mitigation for the sugarcane industry

The objectives of my research were to determine the relationship between the sugarcane burning and increased nitrogen levels and precipitation; to determine if some areas that have more impact by annual burning also have a greater environmental impact

through soil loss; and to provide alternative mitigation options for sustainable change to the traditional field burning practice that will allow for future economic growth of the commercial sugarcane industry.

Background

The Everglades is a vast and unique ecosystem and ancient relic of the once Okeechobean Sea. This large region of subtropical wetlands at one time covered an estimated 4,265 miles^2 (SFWMD, 2021) (2,730,000 acres) compared to the 2,406 miles^2 (1,540,000 acres) as of 2018 (Army, 2018). The Everglades begins north of Lake Okeechobee in the Kissimmee River basin and flows south through Lake Okeechobee and in southeastern direction until the approximate latitude of Miami and turns to the southwest (Figure 1). The water ultimately discharges into the Gulf of Mexico and Florida Bay.

The geomorphology of the Everglades was formed over the past approximately 40 million years with twelve major marine flooding incursions (Petuch & Roberts, 2007). Florida was a large carbonate shelf that extended just south of Georgia to the Florida Straits, under approximately 300-400 meters of water. Carbonate fine silt and sand continued to be deposited over the next 35 million years. The change that resulted in the geologic structure of the Everglades is referred to as the Pseudoatoll Depositional Episode (Petuch & Roberts, 2007). Most notably, the water became warmer, which allowed for reefs and vegetation to grow, and due to major glaciation events, sea level decreased leaving significantly more land exposed. The main geomorphic flow pattern of the Everglades was thereby established.

The sediments found with the Everglades are predominately peat, sand, and limestone. The peat has been deposited during the recent historical period of sawgrass flats. The historical freshwater Everglades (Figure 1) was a slower flowing section which allowed for the fine-grained sediment to accumulate and form a several foot layer of

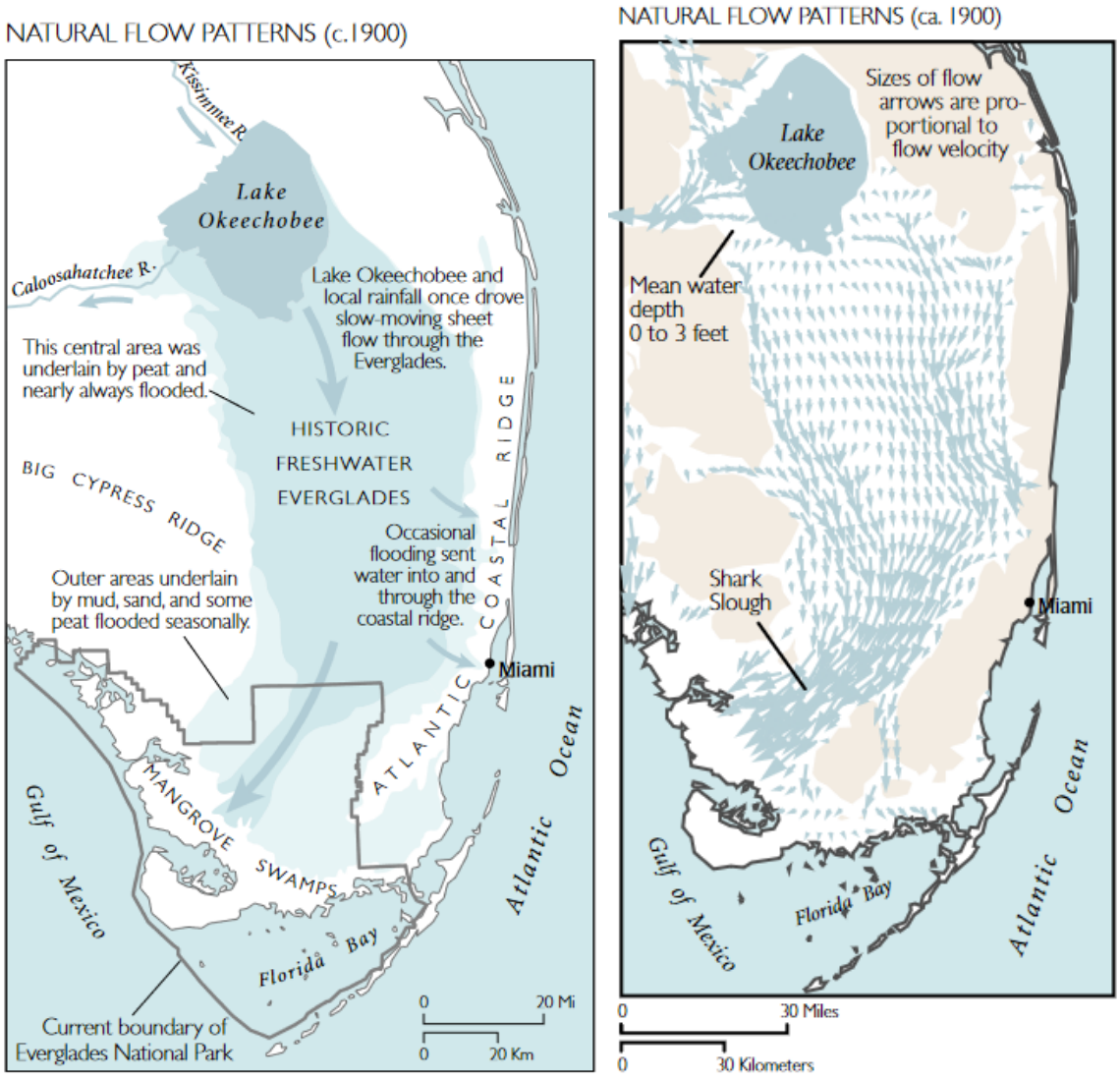

Figure 1. Original flow patterns of the Everglades from Lake Okeechobee.

The left map describes the typical flow patterns of surface water entering Lake Okeechobee through the Everglades and discharging into the Gulf of Mexico. The right map illustrates the flow direction and velocity in greater detail. (USGS, 1999)

highly organic clay and silt, i.e., peat. In areas with faster moving surface water, fine grained sediment was not able to build up and larger grained silicate sands were deposited.

Development of the Everglades

There is a long history of development of the Everglades (Table 1), beginning after the United States Congress passed the Swamp Land Act of 1850. This Act enabled wetlands within the state to be reclaimed for development into agricultural land. Twenty million acres of federal land were transferred to the state of Florida. In 1907, under Governor Napoleon Bonaparte Broward the Everglades Drainage District was established. This district reclaimed large sections of the eastern Everglades for agriculture development via the construction of five major canals.

In 1947 the US Congress established 1.5 million acres of the southern Everglades as the Everglades National Park. Local conservationist Marjory Stoneman Douglas also published her very influential book, *The Everglades: River of Grass* in 1947, bringing national attention to the conservation of the Everglades.

The Central and Southern Florida (C&SF) project was authorized in the Flood Control Act of 1948, by the US Congress, to allow for the construction of water infrastructure improvements, e.g., canals and dikes. These improvements rerouted water for flood control; to supply water for municipal, industrial, and agricultural uses; to prevent saltwater intrusion; to supply water for the Everglades National Park; and to protect fish and wildlife resources. Additionally, the Everglades was subdivided into multiple parts. One of the major sectors created was the EAA.

In 1972, Governor Reubin Askew signed into law the Water Resources Act of 1972. Following this progressive act, the water within Florida is now held in public trust for the benefit of the public. This allowed for the creation of the five Water Management Districts as they are presently. The Clean Water Act was established in 1972 and Florida

Table 1. Timeline of notable events pertaining to the Everglades and sugarcane industry.

YEAR	EVENT	RESULT
1850	United States Congress passes the *Swamp Land Act of 1850*	This allowed wetlands to be used as agriculture land
1907	Everglade Drainage District was established under Gov. Broward	The first major canals were built for further agriculture development
Cir. 1920	The commercial sugarcane industry began in the counties around the south and southeast side of Lake Okeechobee.	Development of tens of thousands of acres into sugarcane farmland.
1947	United States Congress established 1.5 million acres as the Everglades National Park Marjory Stoneman Douglas publishes *The Everglades: River of Grass*.	National attention is brought to the Everglades. The first major conservation effort is done.
1948	United States Congress authorized the Central and Southern Florida project as part of the *Flood Control Act of 1948* The Everglades was subdivided into multiple parts.	This allowed for the construction of infrastructure within the water for the purpose of flood control. The EAA was formally established.
1960	United States embargo on Cuba.	Sugarcane land grew from approx. 50,000 acres to over 400,000 acres over the next few decades.
1972	The *Water Resources Act of 1972* was established under Gov. Askew United States Congress passes *The Clean Water Act*.	This gave the water rights of Florida to the public. This act allowed for the creation of five Water Management Districts. The Clean Water Act was the first federal law to protect water quality.
1977	Florida Congress passes the *Safe Drinking Water Act*.	Florida expands upon federal regulation formally prohibiting

		discharge of waste-water into state water, surface and ground.
1992	United States Congress passes the *Water Resources Development Act of 1992*.	First act passed to improve infrastructure, in part relating to the Everglades
1994	Florida Congress passes the *Florida Everglades Forever Act*.	This act was aimed at reducing phosphorous levels in the Everglades.
1996	United States Congress passes the *Water Resources Development Act of 1996*.	Continuation of infrastructure improvements
2000	United States Congress authorizes the *Comprehensive Everglades Restoration Plan*.	Major legislation that aimed at correcting the flow pattern of water flowing out of Lake Okeechobee back to the original course.
2000	United States Congress passes the *Water Resources Development Act of 2000*.	Continuation of infrastructure improvements
2007	United States Congress passes the *Water Resources Development Act of 2007*.	Continuation of infrastructure improvements
2014	United States Congress passes the *Water Resources Development Act of 2014*.	Continuation of infrastructure improvements
2016	United States Congress passes the *Water Resources Development Act of 2016*.	Continuation of infrastructure improvements
2018	United States Congress passes the *Water Resources Development Act of 2018*.	Continuation of infrastructure improvements
2020	United States Congress passes the *Water Resources Development Act of 2020*.	Continuation of infrastructure improvements

implemented its own guidance in 1977 through the Florida Safe Drinking Water Act. This formally prohibited discharge of waste-water into state water, surface and ground, unless a Water Management District issued a permit to do so.

Over time adjustments were made to improve infrastructure via the Water Resources Development Acts (WRDAs) in 1992, 1996, 2000, 2007, 2014, 2016, 2018, and 2020. In 1994 the Florida Everglades Forever Act was passed to improve water quality within the Everglades by reducing P levels. This expedited the plans and programs for improving water quality via the Everglades Construction Project among others (SFWMD, 2021). In 2000 the US Congress authorized the Comprehensive Everglades Restoration Plan (CERP). The project purpose was to correct, within the limitations of infrastructure, the flow pattern of the water flowing out of Lake Okeechobee to the original course. The original flow direction, as shown in Figure 1, is directly through the commercial sugarcane fields within the EAA and subsequently into the Everglades.

Sugarcane Cultivation in Florida

Sugarcane is a large grass species of the *Saccharum* genus (Brumbley et al., 2009). Annual planting occurs between September and January. Sugarcane is grown in ratoons, i.e., harvested multiple times from a single planting, that take from 12 to 15 months to mature. Harvest is from late September to late April and is dependent on the variety of sugarcane grown. Once the final crop has been harvested after three or four ratoons, the field is tilled to clear it and is either planted with more sugarcane or another rotational crop such as sweet corn, rice or lettuce.

The soil within the EAA is composed of a thick layer of peat, a relic of predevelopment sawgrass flats, which is underlain by limestone (Rice et al., 2005; Qualls & Richardson, 2002). Some fine quartz sand is interbedded between the peat and limestone in the more southern portions of the Everglades (Figure 2). The original peat

layer was several meters thick (Qualls & Richardson, 2002). The peat layer acts as a source of both N and carbon for the sugarcane (Wright, 2019). The fine sand and limestone add minimal nutrients to aid in sugarcane growth and are highly leachable (McCray et al., 2016); i.e., water passes through the soil quickly. As a grass, sugarcane requires more N than any other macronutrient. The peat has been a sustainable source of N for most agriculture in the EAA.

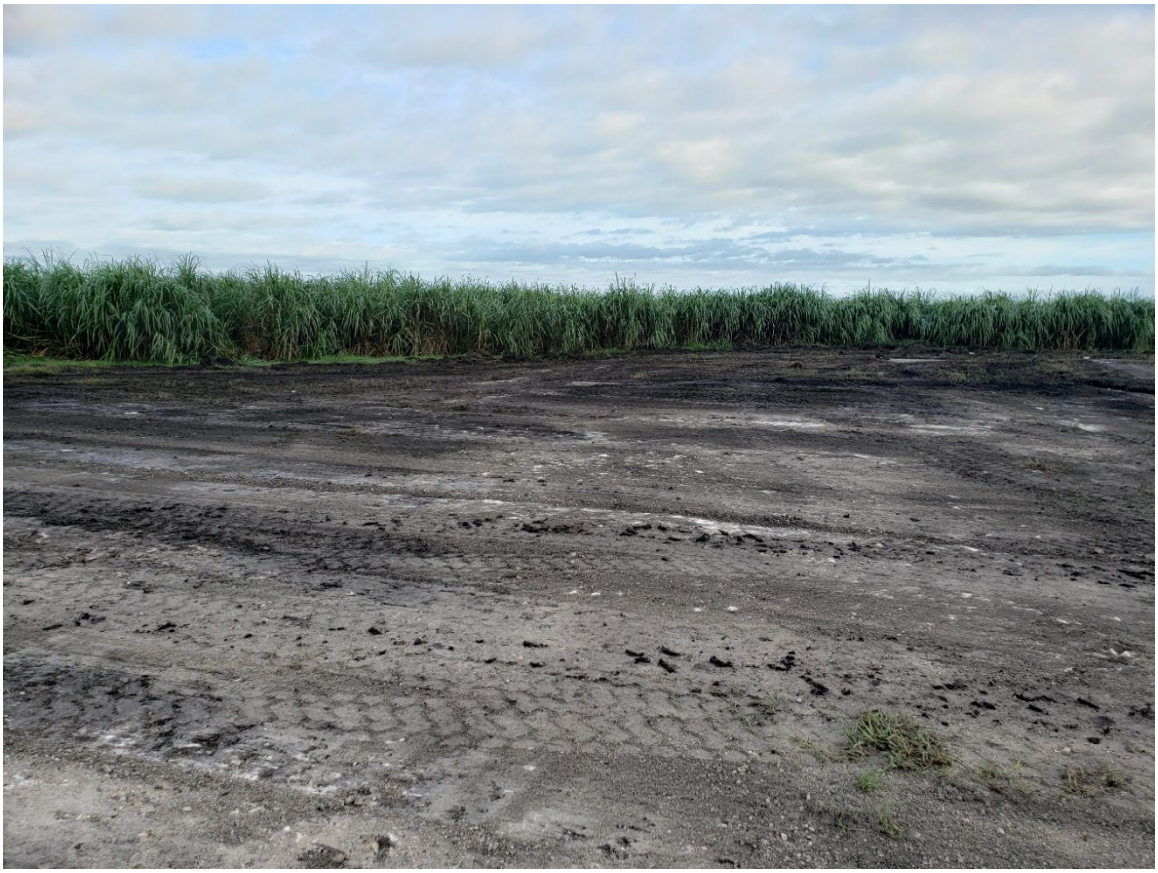

Figure 2. Photograph of sugarcane and organic sandy soil.

Sugarcane in background, with organic sandy soil and some visible limestone rock in foreground. Photo by author within the EAA in 2020.

Over time with successive sugarcane harvests, the original thick peat layer began to break down due to microbial decomposition, oxidation, dry conditions, temperature (Qualls & Richardson, 2008), and burning (Lukenbach et al., 2015), and eroded away at rates exceeding 1-inch per year (Qualls & Richardson, 2008). The sugarcane industry subsequently adjusted their farming practices to mitigate this decay and has slowed the process to approximately 0.5 inch per year (Qualls & Richardson, 2008).

The pre-harvest burn is done in the dry season and as the peat dries out, it becomes more susceptible to burning and subsequent thickness loss (Lukenbach et al., 2015). As the soil decays, the N within peat mineralizes and becomes mobile, along with several other mineral nutrients, (McCray et al., 2019; Wright, 2019). Consequently, N loss occurs and is washed away as agricultural runoff each year, through precipitation and a lesser extent irrigation runoff. Mineralized N contained within the peat accounts for 97%, rainfall 2%, and irrigation water 1% of the total N that enters the EAA, from internally and externally, as runoff at an approximate rate of 780 lb N/acre per 0.5 inches of organic soil (McCray et al., 2019). Minimal peat is prevalent upgradient of the EAA.

Present day cultivating techniques are significantly more advanced than in previous decades, through the use of machinery, modern fertilizers, and water-use efficiency. Irrigation within the EAA is nearly exclusively through interconnected canals. Farms are permitted to pump directly from the canals for use on the fields. There is potential for nutrient recycling and effort is made to reduce fertilization to prevent unnecessary runoff and additional fertilizer costs (Daroub et al., 2011).

Sugarcane Burn Residue

The traditional practice of preharvest burning is a long-standing practice that is meant to remove the green leaves, termed green trash, to allow for a more efficient harvest and processing. It is not a necessary step in harvesting, but is much more economical than non-burning methods, termed green harvesting. Burning of sugarcane incurs a significant loss of nutrients in the recovered burn residue (BR) (Mitchell et al., 2000) and most significantly N. The loss of N has been estimated to be 77-95% in pre- and/or post-harvest burning (Mitchell et al., 2000).

Nitrogen from the sugarcane burn residue mineralizes in sugarcane fields, just as the N in the decaying peat, and leads to much higher amounts of N loss than non-burning methods (Jeong et al., 2012). Multiple studies have analyzed the N loss and retention through various management methods and determined that leaving the green cane trash in place would result in more stable soil and less N loss (Jeong et al., 2012; Ball-Coelho et al., 1993; Thorburn et al. 2004; Bordonal et al., 2018). Thorburn et al. (2004) also stated that the N would become immobilized in a highly organic soil. The quality of organic soil then becomes of greater importance. When the sugarcane is burned, the peat also burns, with the extent based on its density and moisture content (Lukenbach et al., 2015). As the peat burns, additional ash is added to the BR, thus increasing the N content. It should be noted that the interaction of BR and runoff is still poorly understood.

As research into the peat loss and soil stability continued, many farmers have begun rotating crops for soil fixation of C and N, but it is not a widespread industry practice. Additionally, the University of Florida Institute of Food and Agricultural Science (UF IFAS) has conducted extensive research on the sugarcane industry and

maintains a best practices handbook. However, recommendations for the use of N are not given nor required for sugarcane grown on highly organic soils (McCray et al., 2019).

An increase in nitrogen concentration can lead to eutrophication and potential toxicity to aquatic vertebrate and invertebrate species (Kadlec & Wallace, 2009; Saunders & Kalff, 2001). The risk of substantial damage due to N is low, but still present. The SFWMD major efforts to reduce P has also successfully reduced N runoff. From 2005 to 2021, the total N levels were hypothesized to be decreasing due to filtration in the stormwater treatments areas (STAs) (SFWMD, 2021). An area of potential concern, due to potential elevated P, occurs along the canal edges; these impacted areas are already more susceptible to environmental damages due to elevated N (SWWMD, 2021).

In Table 2 and Figure 3, the total N is presented as a comparison of the baseline (1979 to 1993), Phase 1 Restoration (1994 to 2004), Phase 2 Restoration (2005 to 2019), and current levels (2020). Three Water Conservation Areas (WCA-1, WCA-2, and WCA-3) were designated protected areas of natural land, both publicly and privately owned, that are meant to be restored areas of the original Everglades. The WCAs have the boundaries cordoned off with water control to allow for observation and study to determine how to restore natural water flow in the Everglades (SFWMD, 2022). The total N loads include other sources of N, e.g., atmospheric deposition, but those values are estimated to be minimal.

The drastic decrease from Phase 1 to Phase 2 (Table 2) is likely due to the construction of the STAs, discussed below. The missing piece of information is the measurements of total N load and concentration in a downgradient area that did not have an STA constructed. This could illustrate the significance of the STA reduction and

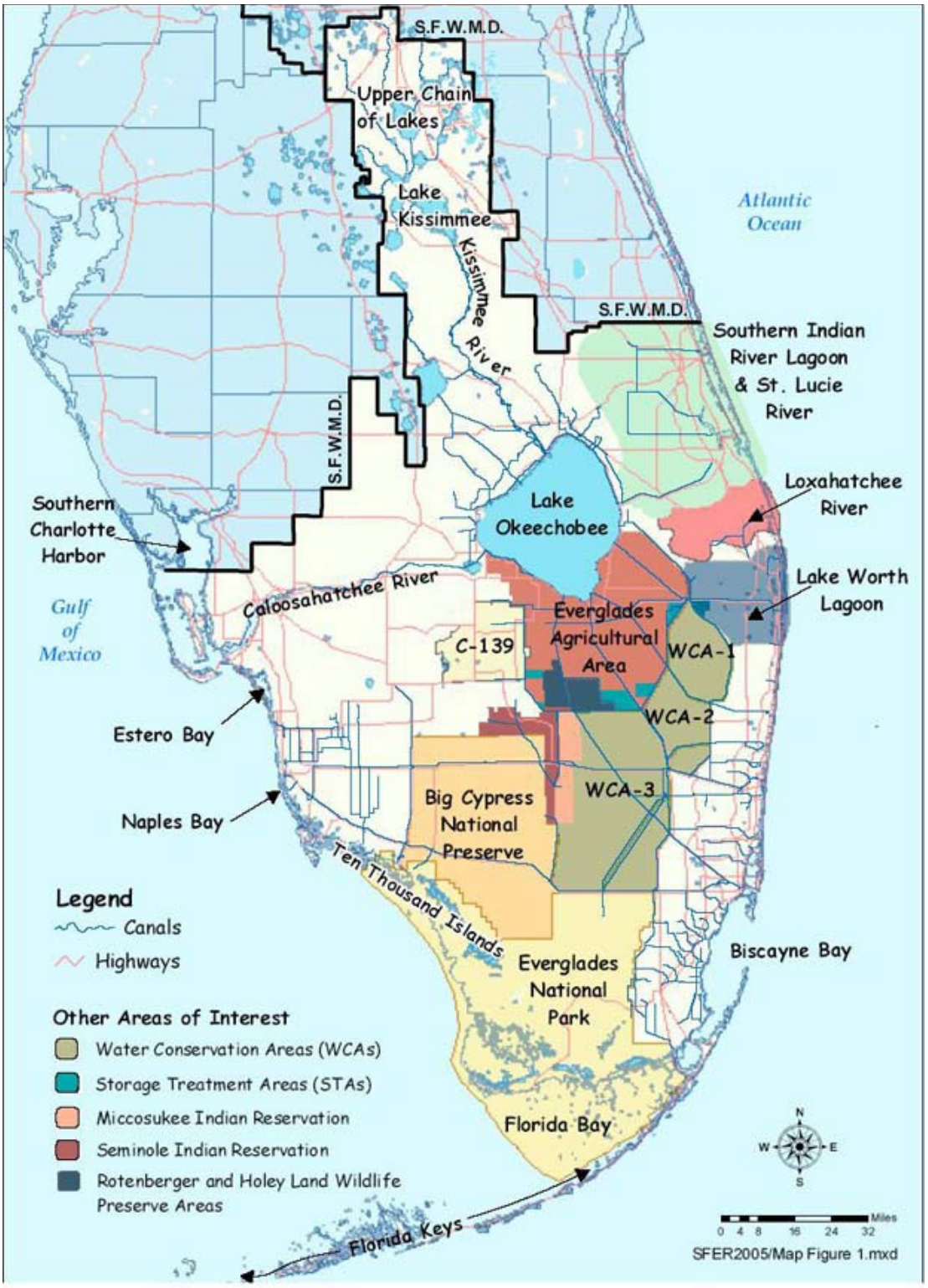

Figure 3. Graphical illustration of the Water Conservation Areas.

Location of the Water Conservation Areas (WCAs), Everglades Agricultural Area (EAA), Everglades National Park, and other various SFWMD designated areas.

Table 2. Total nitrogen loads and water concentrations in the WCAs and Everglades.

Parameter	Location	Baseline 1979-1993	Phase I 1994-2004	Phase 2 2005-2019	Current 2020
Mean Annual Total Nitrogen Load (tons)	Water Conservation Area 1	2983	2610	769	536
	Water Conservation Area 2	2502	2253	1995	1038
	Water Conservation Area 3	3522	3365	2646	2065
	Everglades National Park	1428	1810	1167	1205
Mean Annual Total Nitrogen Concentration Levels (mg/L)	Water Conservation Area 1	5.02	3.16	2.06	1.69
	Water Conservation Area 2	3.77	2.59	1.94	1.71
	Water Conservation Area 3	2.41	1.90	1.57	1.55
	Everglades National Park	1.37	0.98	0.95	1.10

Phase 1 and Phase 2 are the major restoration phases of the Everglades. The table shows the effectiveness of the restoration efforts. My analysis spanned the latter half of Phase 1 and all of Phase 2. Table is modified for clarity from SFWMD, 2021.

show that elevated N levels are still present in the upgradient EAA and continues to be a problem. Figure 4 illustrates the continued impact of N further downgradient of the EAA as the areas closer to the EAA (Figure 3) have higher total N. The graphical depiction of the data shows the spikes that occur annually (Figure 4). If only represented by geometric means, the total N gives the impression of less volatility. The total N was found to have a strong relationship with the total organic carbon and the likely source is the decaying peat (SFWMD, 2021). As discussed previously, the peat erosion has decreased significantly, but continues at a moderately steady pace. This is an additional indication of the terminal nature of the peat decay and erosion.

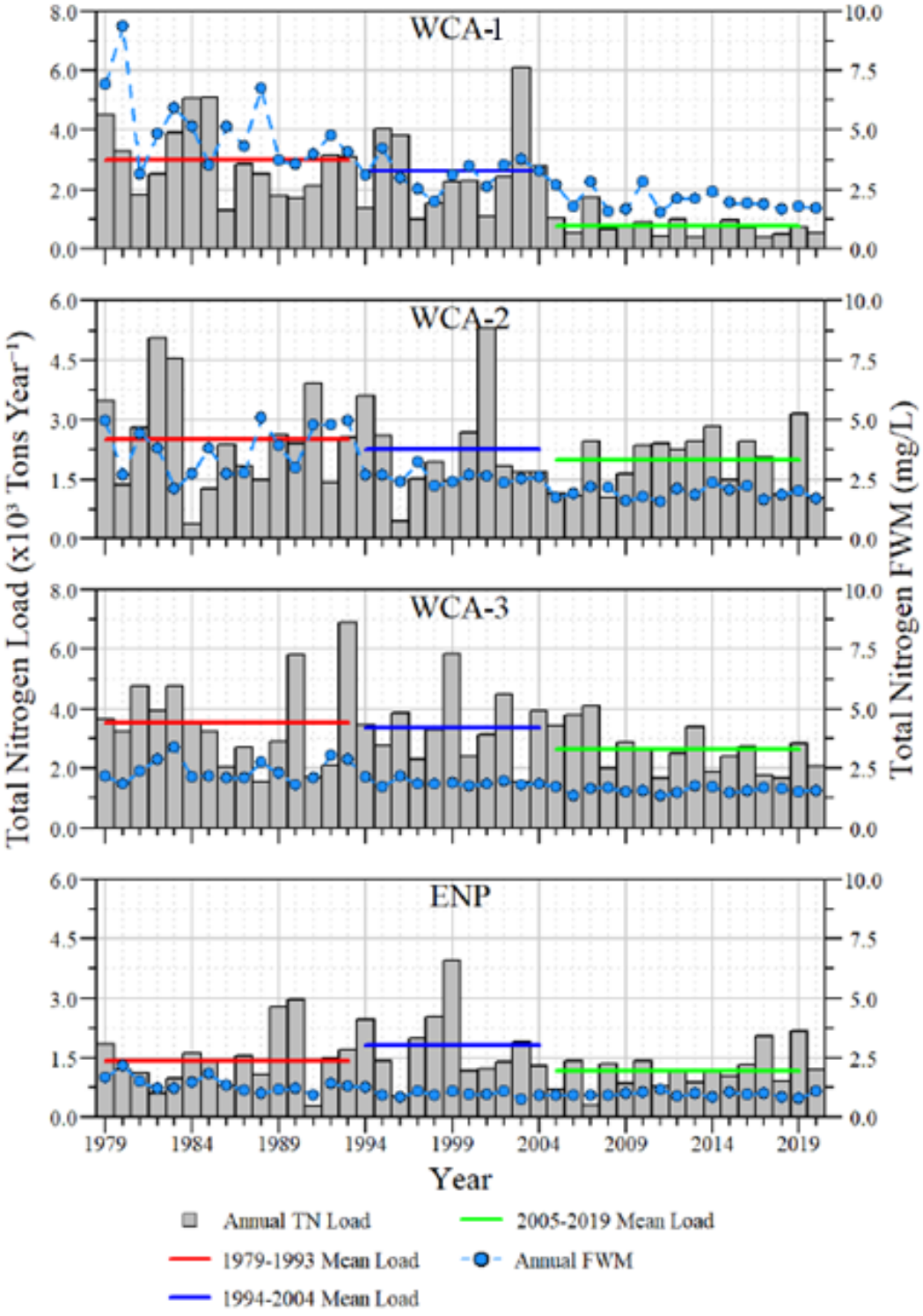

Figure 4. Annual mean total N loads and N concentrations discharged from the WCA-1, WCA-2, WCA-3, and ENP, 1979-2019. The gray bar graphs show the mean total N load per year. The blue dots show the mean total N concentration per year. Figure source SFWMD, 2021.

Monitoring of Water Runoff from the EAA

The SFWMD began monitoring the EAA in the 1970s. This was accomplished by installing strategically placed Water Quality Stations (WQSs). Continuous monitoring of the water quality throughout the Everglades has become a top priority (see Florida Everglades Forever Act, Table 1).

The SFWMD has constructed canal gates throughout the district to manage water levels. The water levels are carefully monitored and are kept at a minimum level for adequate volume to supply the sugarcane farms. Any additional water due to stormwater influx is typically routed to the flow equalization basins (FEB) and STAs located on the southern end of the EAA. The STAs were constructed to allow for high P levels to be naturally mitigated in large, vegetated areas hydraulically confined by canals, before allowing the water to flow into the Everglades Protected Area. Though the STAs were not designed to treat N, they do have some reducing effect (SFWMD, 2020).

The Everglades ecosystem is historically P-limited, so that consequently, minor changes in P cause disproportionately high ecological responses (Julian, 2020). Although the main focus for the SFWMD and Florida Department of Environmental Protection (FDEP) has been on P reduction and not N directly, it has also monitored N (SFWMD, 2021). Additionally, the FDEP has not set a numeric criterion for allowable N levels for outflows from the EEA into surrounding Everglades wetlands; N is only regulated by a narrative criterion: nutrient (e.g., N) concentrations in a water body cannot be altered to cause an imbalance to natural populations of aquatic flora or fauna (Julian et al., 2020).

Research Questions, Hypotheses and Specific Aims

As indicated in Table 2 and Figure 4, the total N levels have fluctuated annually and since sugarcane and precipitation are both seasonal, the monthly N levels likely fluctuate. My research intends to evaluate a possible mechanism for this volatility of N by correlating the N spikes downgradient to the burning that occurs in the sugarcane fields. My research will examine two primary research questions and their associated hypotheses:

1. What is the relationship between the traditional sugarcane practice of pre-harvest burning and nitrogen levels in nearby wetlands?
    - H1: I predict there is a direct correlation between the sugarcane field burning within the EAA and increased nitrogen within the downgradient water, with precipitation as a driving transport mechanism.
    - H1b: I expect to see regional differences between the scale of the burning each year and soil nutrient loss as measured through water quality observations.
2. Can a sustainable change be made to the traditional field burning practice that will allow for future economic growth of the commercial sugarcane industry?
    - H2a: I propose that substantial environmental benefits can be realized by mitigating N impacts by altering sugarcane farming practices to reduce burning.
    - H2b: I expect some of the alternative practices to burning to be cost-effective.

Specific Aims

To address these questions and hypotheses, I needed to:

1. Establish a study area within EAA that is hydraulically confined by major canals.

2. Identify study points within the study to collect data from.
3. Acquire the environmental variable data from permanent monitoring stations owned and operated by the SFWMD.
4. Organize and process the acquired ground station data.
5. Determine the timeframe of the research and make a final selection of specific ground stations to utilize for the statistical analyses.
6. Acquire satellite imagery for remote sensing analyses.
7. Process the satellite imagery to produce the selected spectral indices.
8. Perform a supervised thresholding of the ground cover types in the study area.
9. Correlate the spectral indices with ground station data.
10. Perform data correction and recalculation of the satellite data.
11. Correlate the corrected spectral indices data with ground station data.
12. Create time-series analyses of the acquired corrected satellite imagery.
13. Acquire Climate Engine data from selected regions in the study area.
14. Perform statistical calculations on the Climate Engine data.
15. Analyze the results and determine a relationship between the field burning and the N, and precipitation data.
16. Develop cost-benefit analyses for the purpose of mitigating N and sugarcane sustainability.
17. Present alternative options to preharvest burning and recommend changes to sugarcane best practices based on findings.

These research steps are organized into a flow diagram (Figure 5).

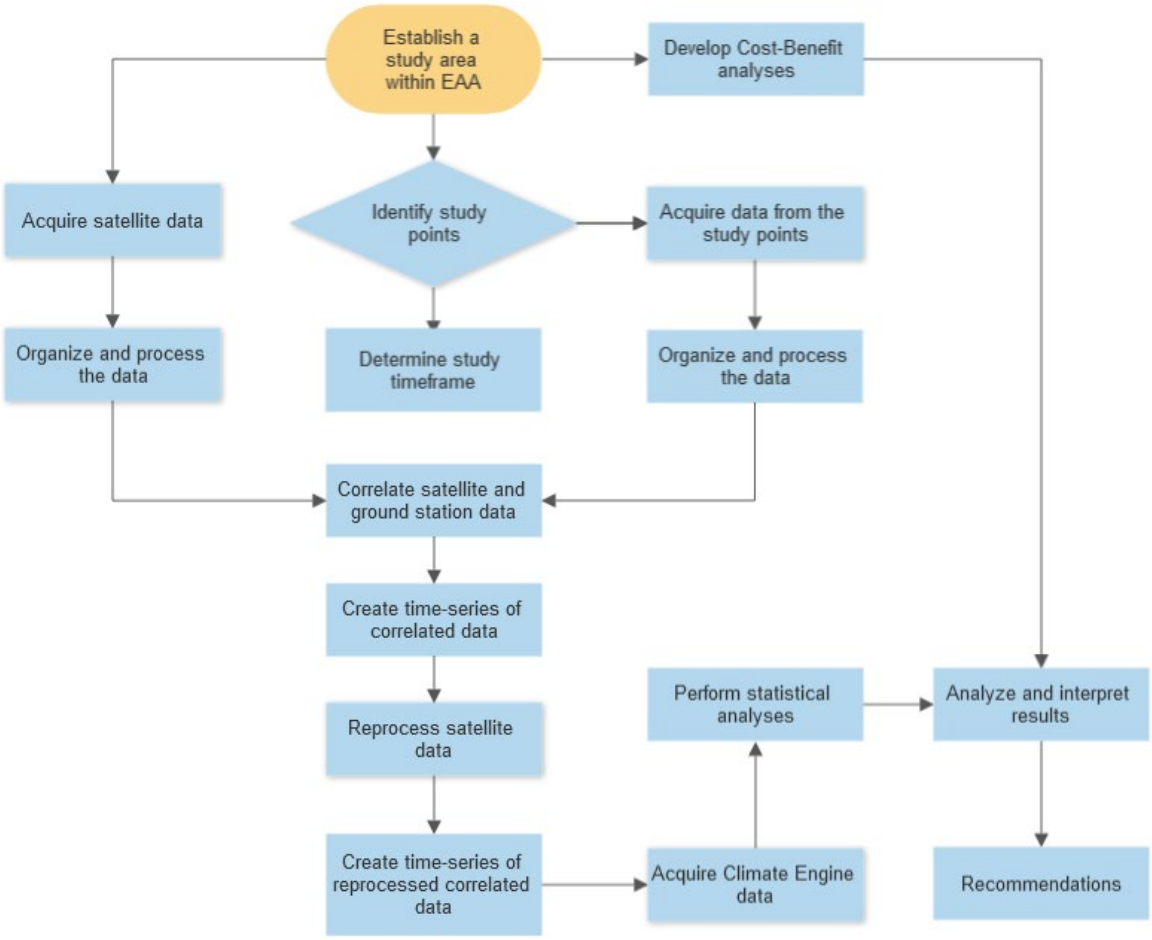

Figure 5. Flow chart of specific aims.

Flow chart illustrating the interconnectivity of various tasks.

Chapter II

Methods

I chose a study area in the EAA that was hydraulically confined that contained minimal non-vegetated surface features, i.e., buildings or roads. A hydraulically confined area is a section of land that has a water feature, in this case the canals, that act as a barrier minimizing water flow through it. The purpose of choosing a hydraulically confined area was to focus on the study area, reducing the influence of the surrounding land. The chosen study area was located in the southern portion of the EAA. The study area limits are defined by the L-15 (Hillsboro Canal), L-16 (Bolles Canal), L-19 (North New River Canal), and L-6 canals (Figure 6). The L-15 and L-19 canals, located on the eastern and western boundaries respectively, are generally oriented in the direction of groundwater flow in the EAA. These canals restrict cross gradient flow which aids in limiting exterior influences on the study area. The northern and southern canals, L-16 and L-6 respectively, were chosen to enclose the study area because this allowed for a large enough surface area to analyze data by geographic region, and because these canals intersect ground stations collecting water chemistry data.

In addition to the study area, 21 study points (SPs) were selected within the study area, as delineated in Figure 6. The SPs are spatially specific data points as opposed to regional data. The SPs are grouped in clusters of three that are located relatively close to each other. The location areas I chose were to representative of the different regions of the study area. The regions are the northwest, northeast, central, south, adjacent to station G434, adjacent to station G328, and adjacent to station S6. The four geographically

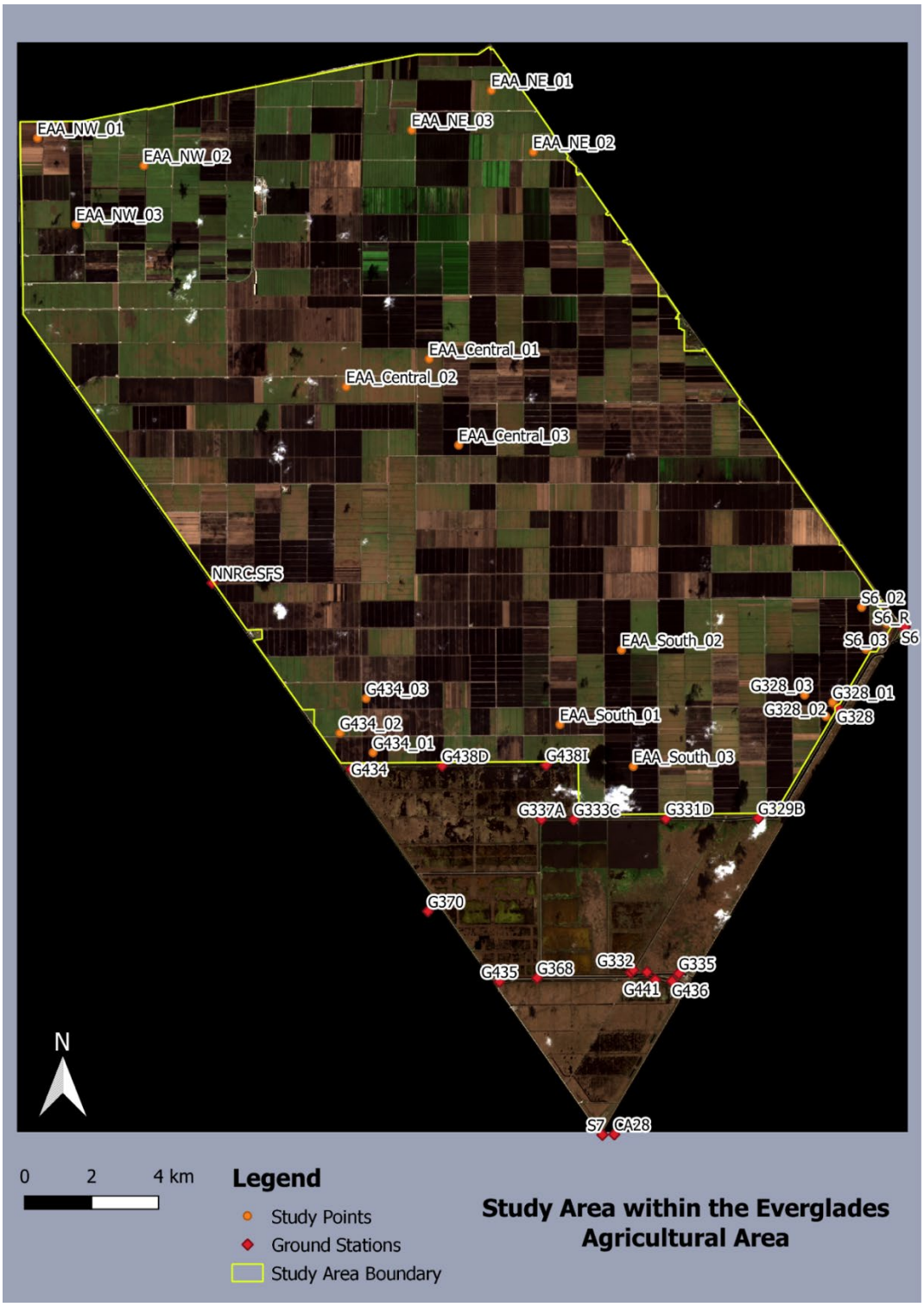

Figure 6. Study area map with study points and ground stations.

Location of all the SPs and ground stations. The delineating marker of the study area is shown in yellow. Many of the ground stations were outside of the study area to the south.

defined regions were specifically identified as active sugarcane growing and harvesting areas. The three ground station regions were chosen due to abundant data present at those specific stations. The individual points were chosen randomly and required to be located on sugarcane, not roads, buildings, or water. The chosen locations also needed to be at least 30 meters from the excluding features. This additional step was to ensure those excluded features were not part of the LandSat pixels, discussed in further detail below.

Ground Station Data

The initial step was to locate chemistry data for the surface water within the EAA. The South Florida Water Management District (SFWMD) publishes an active database of all ground stations throughout the district (Figures 6 & 7). The ground stations are located within the canals, which differs significantly from the SPs. The data collected from the ground stations is not a direct measurement of activity within the sugarcane, but rather data that has collected after a time lapse, i.e., the particular measurement taken only occurs after the water has traveled from the land surface into the canal, down the canal and through the ground station. I identified dozens of stations downgradient of my study area. These stations were selectively reduced based on available data, type of data, and time-frame. The final list of relevant ground stations to my study area, by proximity, included nineteen (19) down gradient and three (3) upgradient (Table 3).

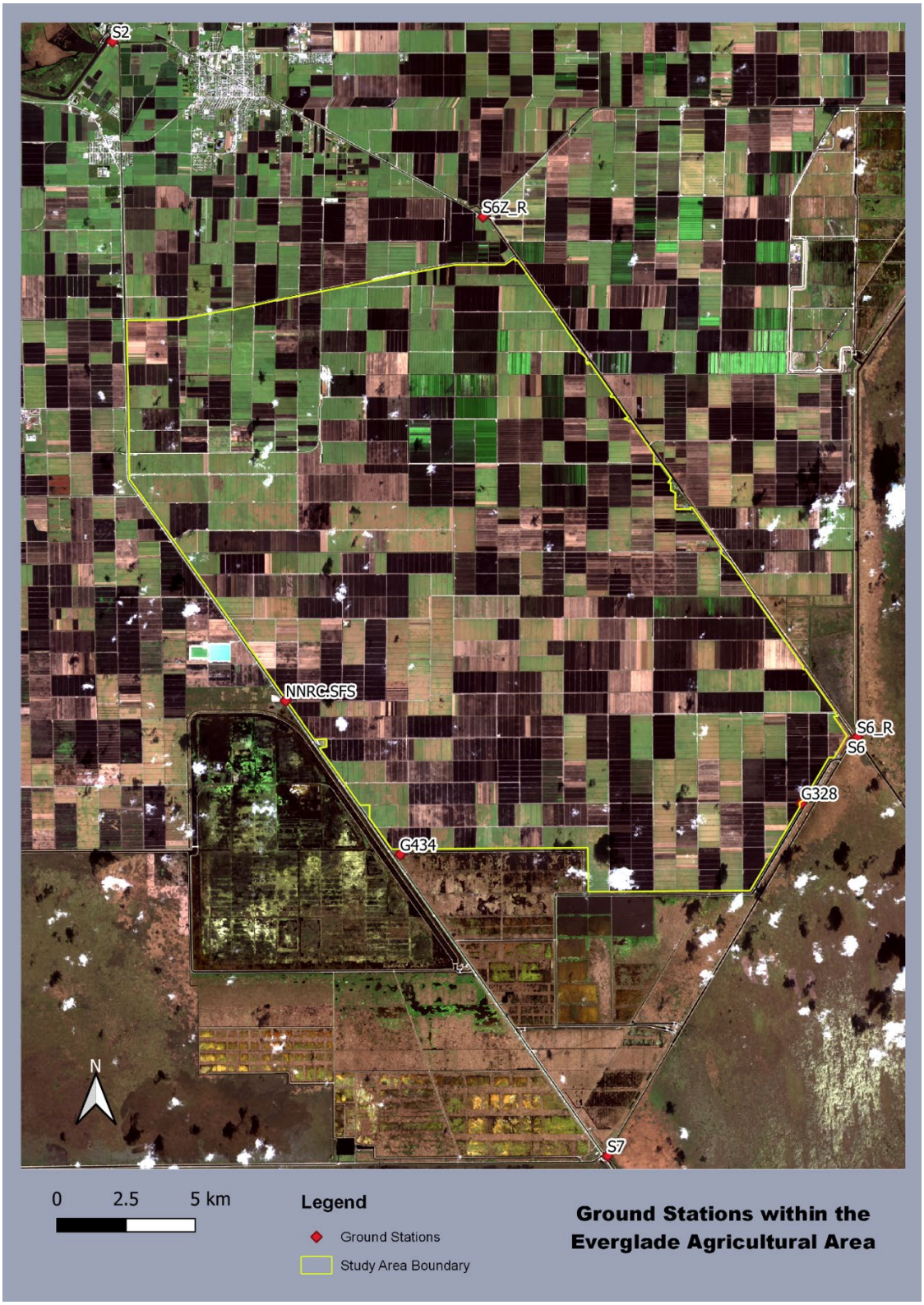

Figure 7. Study area and ground stations within the EAA.

A map showing the location of the selected ground stations utilized in this thesis.

Table 3. Ground station categorization.

	Down Gradient Points							
	Station ID	Date		Time Span (Days)	Time Span (Years)	Constituent	Data Gaps	Gap Comment
		Start	End					
G328	G328	2001-03-14	2021-04-28	7,350	20.14	Nitrate+Nitrite-N	NO	
	G328	2001-03-14	2010-06-02	3,367	9.22	Nitrate-N	YES	2005, 2008
	G328	2001-03-14	2007-09-12	2,373	6.50	Nitrite-N	NO	
	G328	2019-11-06	2019-11-06	0	0	Nitrogen, Total Dissolved	NO	
	G328	2015-11-24	2021-04-28	1,982	5.43	Total Nitrogen	NO	
G329B	G329B	2002-02-13	2012-12-27	3,970	10.88	Nitrate+Nitrite-N	NO	
	G329B	2009-01-28	2010-06-02	490	1.34	Nitrate-N	NO	
G330D	G330D	2005-06-08	2020-02-26	5,376	14.73	Nitrate+Nitrite-N	YES	2013-2018
	G330D	2009-01-14	2010-05-19	490	1.34	Nitrate-N	NO	
	G330D	2019-11-20	2019-11-20	0	0	Nitrite-N	NO	
	G330D	2019-11-20	2020-02-26	98	0.27	Total Nitrogen	NO	
G331D	G331D	2002-02-27	2012-12-27	3,956	10.84	Nitrate+Nitrite-N	NO	
	G331D	2009-01-14	2010-06-02	504	1.38	Nitrate-N	NO	
	G331D	2002-02-27	2002-07-03	126	0.35	Nitrite-N	NO	
G332	G332	2002-05-22	2019-11-13	6,384	17.49	Nitrate+Nitrite-N	YES	2013-2018
	G332	2009-01-14	2010-06-02	504	1.38	Nitrate-N	NO	
	G332	2004-08-04	2004-08-04	0	0	Nitrite-N	NO	
	G332	2019-11-13	2019-11-13	0	0	Total Nitrogen	NO	
G333C	G333C	2002-08-14	2012-12-27	3,788	10.38	Nitrate+Nitrite-N	NO	
	G333C	2009-01-14	2010-06-02	504	1.38	Nitrate-N	NO	
G334	G334	2001-06-20	2019-04-10	6,503	17.82	Nitrate+Nitrite-N	YES	2013-2018
	G334	2007-01-31	2010-05-19	1,204	3.30	Nitrate-N	YES	2008
	G334	2001-06-20	2007-10-10	2,303	6.31	Nitrite-N	YES	2002-2009
	G334	2019-04-10	2019-04-10	0	0	Nitrogen, Total Dissolved	NO	
	G334	2019-04-10	2019-04-10	0	0	Total Nitrogen	NO	
G335	G335	2001-03-14	2021-05-05	7,357	20.16	Nitrate+Nitrite-N	NO	
	G335	2001-03-14	2010-06-02	3,367	9.22	Nitrate-N	YES	2005, 2008
	G335	2001-03-14	2007-09-12	2,373	6.50	Nitrite-N	NO	
	G335	2019-02-27	2019-02-27	0	0	Nitrogen, Total Dissolved	NO	
	G335	2015-07-22	2021-05-05	2,114	5.79	Total Nitrogen	NO	
G377A	G337A	2008-01-16	2012-10-30	1,749	4.79	Total Nitrogen	YES	2011
	G337A	2009-01-14	2010-06-02	504	1.38	Nitrate-N	NO	

G368	G368	2008-01-16	2019-09-11	4,256	11.66	Nitrate+Nitrite-N	YES	2011, 2013-2017
	G368	2009-01-14	2010-06-02	504	1.38	Nitrate-N	NO	
	G368	2018-11-14	2019-09-11	301	0.82	Total Nitrogen	NO	
G370	G370	2004-03-11	2021-05-03	6,262	17.16	Nitrate+Nitrite-N	NO	
	G370	2009-01-20	2010-05-24	489	1.34	Nitrate-N	NO	
	G370	2014-08-04	2021-05-03	2,464	6.75	Total Nitrogen	NO	
G434	G434	2012-09-06	2021-05-12	3,170	8.68	Nitrate+Nitrite-N	NO	
	G434	2015-11-24	2021-05-12	1,996	5.47	Total Nitrogen	NO	
G435	G435	2012-09-06	2021-05-12	3,170	8.68	Nitrate+Nitrite-N	NO	
	G435	2015-12-03	2021-05-12	1,987	5.44	Total Nitrogen	NO	
G436	G436	2012-09-06	2021-05-05	3,163	8.67	Nitrate+Nitrite-N	NO	
	G436	2015-11-24	2021-05-05	1,989	5.45	Total Nitrogen	NO	
G438D	G438D	2012-05-16	2019-02-13	2,464	6.75	Nitrate+Nitrite-N	YES	2013, 2014, 2016, 2017
	G438D	2018-10-24	2019-02-13	112	0.31	Total Nitrogen	NO	
G438I	G438I	2012-05-16	2019-03-27	2,506	6.87	Nitrate+Nitrite-N	YES	2013-2018
	G438I	2019-01-30	2019-03-27	56	0.15	Total Nitrogen	NO	
G441	G441	2011-11-03	2018-12-05	2,589	7.09	Nitrate+Nitrite-N	YES	2014-2017
	G441	2018-12-05	2018-12-05	0	0	Total Nitrogen	NO	
S6	S6	1974-06-10	2021-04-28	17,124	46.92	Nitrate+Nitrite-N	NO	
	S6	1974-06-10	2010-06-02	13,141	36.00	Nitrate-N	NO	
	S6	1974-06-03	2009-07-01	12,812	35.10	Nitrite-N	NO	
	S6	2014-09-03	2021-04-28	2,429	6.65	Nitrogen, Total Dissolved	NO	
	S6	2014-09-03	2021-04-28	2,429	6.65	Total Nitrogen	NO	
S7	S7	1974-06-10	2021-05-04	17,130	46.93	Nitrate+Nitrite-N	NO	
	S7	1974-06-10	2019-11-19	16,598	45.47	Nitrate-N	YES	2011
	S7	1974-06-03	2021-05-04	17,137	46.95	Nitrite-N	YES	2010, 2011
	S7	2014-10-06	2021-05-04	2,402	6.58	Nitrogen, Total Dissolved	NO	
	S7	2014-09-15	2021-05-11	2,430	6.66	Total Nitrogen	NO	

Complete table illustrating ground station categorization, specifically based on nitrogen. These are ground stations determined to be relevant based on proximity to the study area.

A focal point of this thesis is nitrogen, so I downloaded up to five nitrogen analyses performed: nitrate+nitrite-N (N+N), nitrate-N, nitrite-N, total dissolved

nitrogen, and total nitrogen, if available at each ground station. The N variables downloaded for each ground station is shown in Table 3. Nitrate (NO_3) is the most common form of nitrogen found in groundwater and common in soil. Nitrite ($NO_{2)}$ is not typically present in natural systems and converts to nitrate in groundwater due to it being a less stable compound. Both nitrogen compounds are generally associated with septic systems, fertilizers, and other organic sources as surface runoff. Total nitrogen is the sum of all nitrogen forms. Testing for total nitrogen is typically not as common, compared to other nitrogen compound tests, due the inclusion of naturally occurring compounds that can skew the results. Total dissolved nitrogen is the same as total nitrogen except the sample was filtered to remove sediment as a way to minimize false positives deriving directly from nitrogen compounds within the sediment. In this study, the Nitrate+Nitrite-N (nitrate plus nitrite compounds) was the most common form of N tested because it covers only the nitrate and nitrite compounds, which are both regulated by the US EPA, and does not include organic forms of nitrogen nor ammonia. Organic nitrogen and ammonia are typically from different sources and are tested for separately.

The downloaded data needed very little processing, e.g., duplicate sample data (for quality control/assurance purposes), malfunctioned analyzer data (noted in the sample notes), adjusting negative data to 0 (so long as the margin of error was the reported value, otherwise the data point was removed as an erroneous point), removal of unneeded information relating to the sampling and station.

The data were then organized chronologically by chemical constituent (Table 3). I created an overview of what each ground station's data covered. The ground stations were categorized based on time-frame of the data, chemical constituents analyzed for,

and data gaps within the series (Table 3). After inspecting the data overview chart, I determined N+N had the longest continuous coverage with the most data points. This was true at multiple ground station locations. This allowed me to reduce the number of relevant ground stations to three main locations to focus on. Additional ground stations could be included if needed, but the proximity was too far and/or data set, for N+N, was not continuous or the data set was too small.

In addition, precipitation data was downloaded from three ground stations, S6Z_R, S6_R, and NNRC.SFS, chosen to cover the upper portion, S6Z_R, the central portion, NNRC.SFS, and southern portion of the study area, S6_R (Figure 7). The precipitation ground stations were separate stations from the ones collecting water samples. The precipitation data were collected on a daily basis and were continuous from the early 1990s to present day, but only data from 2000-2020 was retained.

LandSat Data

High resolution satellite images of the study area were acquired from the United States Geological Survey (USGS) EarthExplorer database. This is an online database of archived satellite images of the Earth's surface. The image products chosen for my research were the LandSat 8 Operational Land Imager (OLI) and Thermal Infrared Sensor (TIRS) Collection 2 Level-1, Tier 1 (T1). As described in the USGS 2019 *LandSat Collection 1 Level 1 Product Definition*, the T1 images are the highest resolution, and the most suitable for time-series analysis. The LandSat 8 satellite has a temporal resolution, or time gap, of 16 days between images at a specific location.

I began by performing an exploratory phase of the available data, limiting the initial baseline timeframe from 2018-2020. The data were manually processed and manipulated, which was a very time-consuming process. The limited data set served as a way to familiarize myself with the data and trends. I worked with only LandSat 8 during this exploratory phase due to availability of continuous data (i.e., no large gaps due to cloud cover) and higher quality imagery (Table 4). The specific range in years were chosen at random.

Initial Analysis of Spectral Indices

Once I acquired the LandSat 8 data from 2018-2020 for the study, I calculated the normalized difference vegetation index (NDVI) and normalized burn ratio (NBR) for each image. To accomplish this, I utilized the open-source geographic information system (GIS) software QGIS, version 3.16. GIS programs are graphical interface software that displays map images, as layers, and allows for georeferencing and manipulation of the digitized image with geographical and non-geographical data.

The first step was to create the vector file of my study area. The vector file was georeferenced to the specific latitude and longitude coordinates of the surrounding canals. The purpose of the vector was to allow cropping of the very large satellite images down to only the study area, thus removing erroneous or irrelevant data. The LandSat image files for each date are divided into light wavelength bands. The bands for LandSat 8 are described in Table 5.

Table 4. LandSat cloud cover percentage.

LandSat Cloud Cover Percentage			
Date	**% Total Cloud Cover**	**% Cloud Cover over Land**	**Classification**
1/13/2018	16.18	8.71	Minimal Clouds
1/29/2018	55.18	54.05	Partly Cloudy
2/14/2018	19.56	26.12	Partly Cloudy
3/2/2018	10.65	14.60	Minimal Clouds
3/18/2018	12.10	15.37	Partly Cloudy
4/3/2018	15.74	20.43	Partly Cloudy
4/19/2018	3.91	1.59	Minimal Clouds
5/5/2018	46.59	58.99	Partly Cloudy
6/6/2018	15.55	14.19	Minimal Clouds
6/22/2018	42.66	41.00	Partly Cloudy
7/8/2018	46.25	28.47	Partly Cloudy
7/24/2018	48.23	61.66	Cloudy
8/9/2018	12.43	13.83	Minimal Clouds
8/25/2018	72.58	65.28	Cloudy
9/10/2018	78.70	71.12	Cloudy
9/26/2018	13.19	18.56	Partly Cloudy
10/12/2018	24.29	31.55	Partly Cloudy
10/28/2018	19.52	11.03	Minimal Clouds
11/13/2018	29.25	35.75	Partly Cloudy
11/29/2018	40.14	47.47	Partly Cloudy
12/15/2018	68.17	81.10	Cloudy
12/31/2018	34.97	45.60	Partly Cloudy
1/16/2019	10.27	6.02	Minimal Clouds
2/1/2019	54.40	62.77	Cloudy
2/17/2019	10.00	13.51	Minimal Clouds
3/5/2019	18.97	17.83	Partly Cloudy
3/21/2019	40.61	32.07	Partly Cloudy
4/6/2019	17.54	26.13	Partly Cloudy
4/22/2019	19.18	16.82	Partly Cloudy
5/8/2019	34.15	32.80	Partly Cloudy
5/24/2019	27.46	16.74	Partly Cloudy
6/9/2019	74.77	78.07	Cloudy
6/25/2019	12.38	12.50	Minimal Clouds
7/11/2019	70.26	79.08	Cloudy
7/27/2019	29.51	15.21	Partly Cloudy
8/12/2019	43.41	45.80	Partly Cloudy

8/28/2019	10.27	12.94	Minimal Clouds
9/13/2019	32.33	42.12	Partly Cloudy
9/29/2019	33.87	43.71	Partly Cloudy
10/15/2019	19.96	15.85	Partly Cloudy
10/31/2019	17.49	23.01	Partly Cloudy
11/16/2019	25.76	19.40	Partly Cloudy
12/2/2019	30.34	30.03	Partly Cloudy
1/3/2020	27.93	44.15	Partly Cloudy
1/19/2020	8.76	9.23	Minimal Clouds
2/4/2020	15.86	18.53	Partly Cloudy
2/20/2020	25.02	30.88	Partly Cloudy
3/7/2020	19.97	6.69	Minimal Clouds
3/23/2020	46.39	48.56	Partly Cloudy
4/8/2020	14.89	20.69	Partly Cloudy
4/24/2020	52.02	46.58	Partly Cloudy
5/10/2020	100.00	100.00	Cloudy
5/26/2020	83.77	79.10	Cloudy
6/11/2020	46.42	65.18	Cloudy
6/27/2020	16.79	9.66	Minimal Clouds
7/13/2020	45.03	31.56	Partly Cloudy
7/29/2020	31.70	28.30	Partly Cloudy
8/14/2020	22.76	27.51	Partly Cloudy
8/30/2020	37.96	31.33	Partly Cloudy
9/15/2020	19.10	24.51	Partly Cloudy
10/1/2020	37.48	34.47	Partly Cloudy
10/17/2020	41.86	25.00	Partly Cloudy
11/18/2020	18.15	12.43	Minimal Clouds
12/4/2020	87.19	87.10	Cloudy
12/20/2020	20.76	20.57	Partly Cloudy

Table showing the cloud cover percentage from the LandSat data. This percentage is based on the full-sized image rather than the cropped image I utilized for my calculations. Some dates listed above we not used in the indices calculations due to excessive cloud cover and reliable values could not be ascertained. The classification divisions are arbitrarily and subjectively selected for my own ease of reference.

Table 5. LandSat 8 bands.

Landsat-8 OLI and TIRS Bands (µm)		
Band 1	30 m Aerosol	0.435 - 0.451
Band 2	30 m Blue	0.452 - 0.512
Band 3	30 m Green	0.533 - 0.590
Band 4	30 m Red	0.636 - 0.673
Band 5	30 m NIR	0.851 - 0.879
Band 6	30 m SWIR-1	1.566 - 1.651
Band 7	30 m SWIR-2	2.107 - 2.294
Band 8	15 m Pan	0.503 - 0.676
Band 9	30 m Cirrus	1.363 - 1.384
Band 10	*100 m TIR-1*	10.60 - 11.19
Band 11	*100 m TIR-2*	11.50 - 12.51

Description of the wavelengths for each band captured by LandSat 8.

Prior to importing the images into QGIS, the individual bands for a single date were processed to remove atmospheric haze utilizing the dark-object subtraction (DOS), specifically DOS1, the atmospheric correction tool within the Semi-Automatic Classification Plugin. The DOS1 tool converted each band image into a land surface reflectance image. Land surface reflectance is an image that has been processed to remove the effects of the atmosphere. Moran et al. (1992) described land surface reflectance as:

$$\rho = \frac{[\pi \times (L_\lambda - L_p) \times d^2]}{[T_v] \times ((ESUN_\lambda \times \cos\theta_s \times T_z) + E_{down})]}$$

where:

- L_p is the path radiance

- T_v is the atmospheric transmittance in the viewing direction
- T_z is the atmospheric transmittance in the illumination direction
- E_{down} is the downwelling diffuse irradiance

The DOS1 is a set of specific atmospheric corrections that make specific assumptions about the way light scatters and reflects. The final result of the correction produces an output of each band that has been numerically adjusted based on the aerosol band, Band 1, thus resulting in a clearer image with less interference from the atmosphere.

The next step was to import only the atmospheric corrected bands I needed for calculations of indices and false color composites, and omit the rest. I included Band 2 (blue visible light), Band 3 (green visible light), Band 4 (red visible light), Band 5 (near infrared light [NIR]), Band 6 (shortwave infrared 1 [SWIR-1]), and Band 7 (shortwave infrared 2 [SWIR-2]). Since the thermal and panchromatic bands were not needed in any future work, they were omitted. The six bands were combined into a single image, via raster merging, often referred to as image stacking. Each of the individual bands were placed into separate bands within the single stacked image. This allows for easier processing of each individual date and I was able to display the image using three of the bands for visual inspection in true or false color. True color is utilizing the red, green, and blue bands only to display an image as it would appear normally. False color is utilizing any of the other bands or displaying the red, green, and blue bands in a different order than would occur in nature.

The next steps were to use the stacked images to produce NDVI and NBR images. The NDVI is an index that utilizes the near infrared and red bands. The healthy

sugarcane will have very high reflectance of near infrared and high reflectance of red (Wegmann, Leutner, & Dech, 2016). The NDVI values distinguish when the sugarcane is healthy and dense and when the sugarcane is sparse or freshly harvested. The NBR is not a vegetation index, rather it is a spectral index that focuses on increasing reflective response of the shortwave infrared band and the decreasing reflective response of the near infrared band over burned land. The curves in Figure 8 illustrate the approximate wavelength that ideally is used for the NDVI and NBR calculations, approximately 0.68 (red), 0.8 (near infrared), and 1.6 or 2.2 (shortwave infrared 1 or 2, respectively).

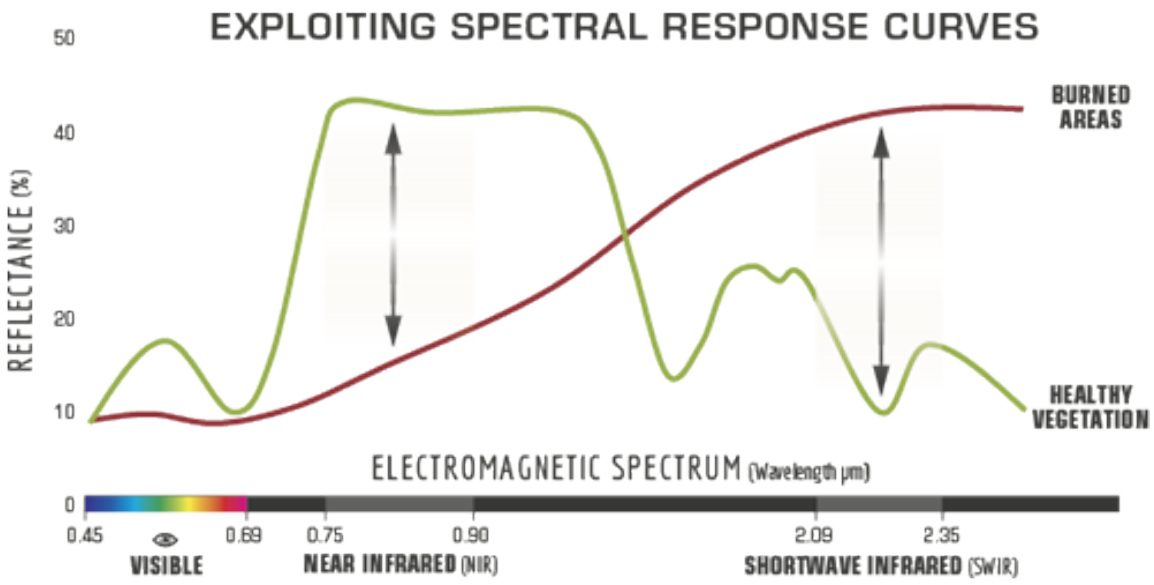

Figure 8. Spectral response graph.

United States Forest Service illustration of spectral responses in vegetation and burned areas. Note that the healthy vegetation and burned areas lines' slopes are positive at the Red and NIR bands.

I used the built-in raster calculator tool in QGIS with the following equations:

$$NDVI = \frac{(NIR - Red)}{(NIR + Red)}$$

$$NBR = \frac{(NIR - SWIR1)}{(NIR + SWIR1)}$$

I calculated the NDVI for each image first, then calculated the NBR. Upon completion of the calculations, I performed a supervised classification of the ground cover types, identifying and classifying each ground cover type based on my field observation and visual inspection of each imported image. Based on this classification, I assigned numerical NDVI value ranges, termed thresholding (Table 6). The values were based on inspecting multiple arbitrary locations for each classification type and identifying the individual features for each and their corresponding pixel values. For each selected location, images were inspected for at least six different randomly selected dates from 2018-2020 to increase my accuracy of classification.

Table 6. Supervised thresholding NDVI values.

Supervised Thresholding of Ground Cover for NDVI		
0	0.21	cloud, building
0.22	0.34	fresh burned ground
0.35	0.46	exposed peat
0.47	0.59	suspected fallowed field
0.6	0.71	growing field
0.72	0.86	sugarcane

Table showing the NDVI value range for each ground cover type

The next step was to export the NDVI and NBR data. This was accomplished by using the Temporal/Spectral Profile (TSP) tool. The TSP tool enabled a graphical and

tabular display of the individual pixel value at each SP location. Within the table view, the data could be copied, i.e., exported, and pasted in an Excel workbook. To collect the entirety of data at a single SP location, every image within the 2018-2020 range was added to TSP tool. Once the data had been copied into the Excel workbook, a cursory graph of each NDVI vs NBR was plotted.

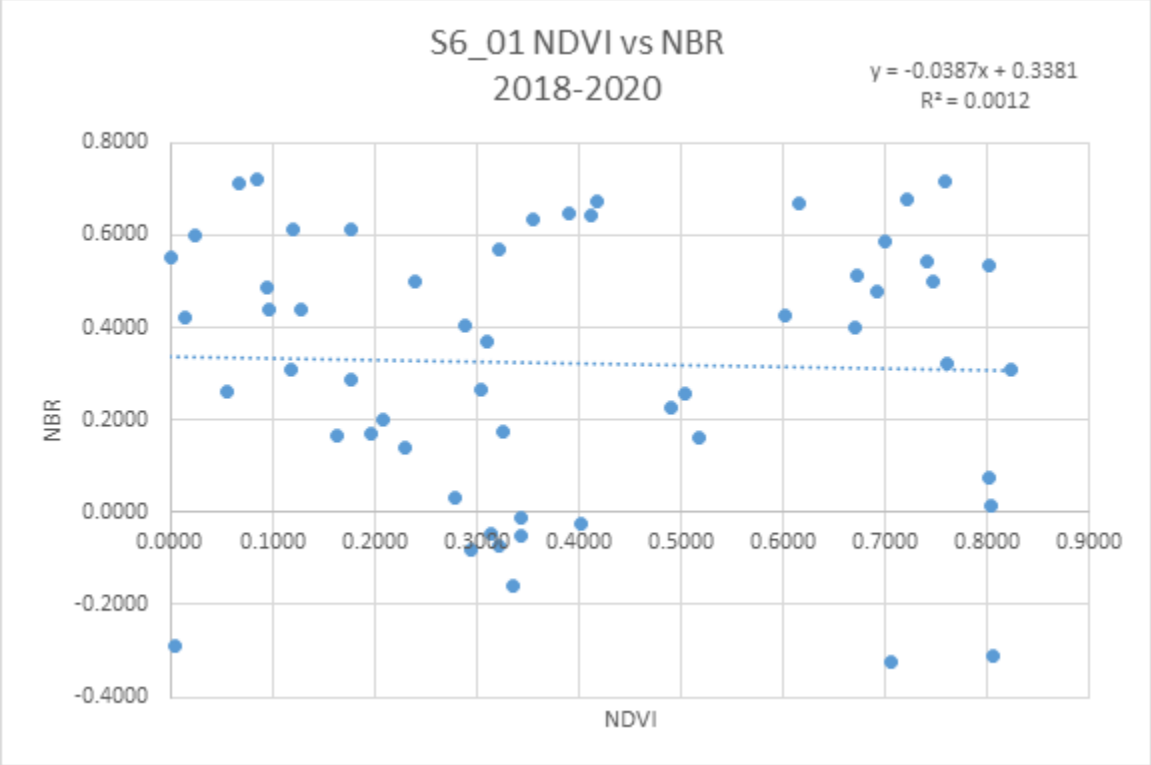

Figure 9. S6_01 NDVI vs NBR graph.

First graphical comparison of NDVI and NBR from 2018 to 2020 at the S6 SP location. The data shows little to no correlation, R^2=0.0012. The dataset included multiple outlying data points.

The initial graphing of the NDVI and NBR showed very poor correlation (Figure 9). Upon inspection of the data used in the graph, multiple values were noted that

included non-sugarcane field data, e.g., clouds, cloud shadows, in the calculation, representing a source of error.

Data Correction and Recalculation

To address the inclusion of erroneous data and to increase the dataset, I reinspected each SP location in the set of 2018-2020 LandSat 8 images. I observed that cloud coverage at the SPs had been included in the statistics. The values for clouds in the NDVI and NBR images were skewing the results. To address this and to not completely dismiss a data point, I adjusted the locations of SPs. Adjustment of an SP location was restricted to a shift within the same field. If the SP remained in the same field, normal agricultural processes would be same at either location, with the vegetation assumed to remain the same throughout a single field; based on my visual inspection of the sugarcane fields, I observed this to be accurate. If an entire field was determined to be unsuitable for a SP shift in location, the data was left empty. This manual adjustment was performed on all 1,155 data points from 2018 to 2020 for the 21 SPs. The data were exported as before using the TSP tool.

Following this data correction protocol, NDVI and NBR was graphed again, indicating the strong correlation ($R^2 = 0.862$) between the variables (Figure 10).

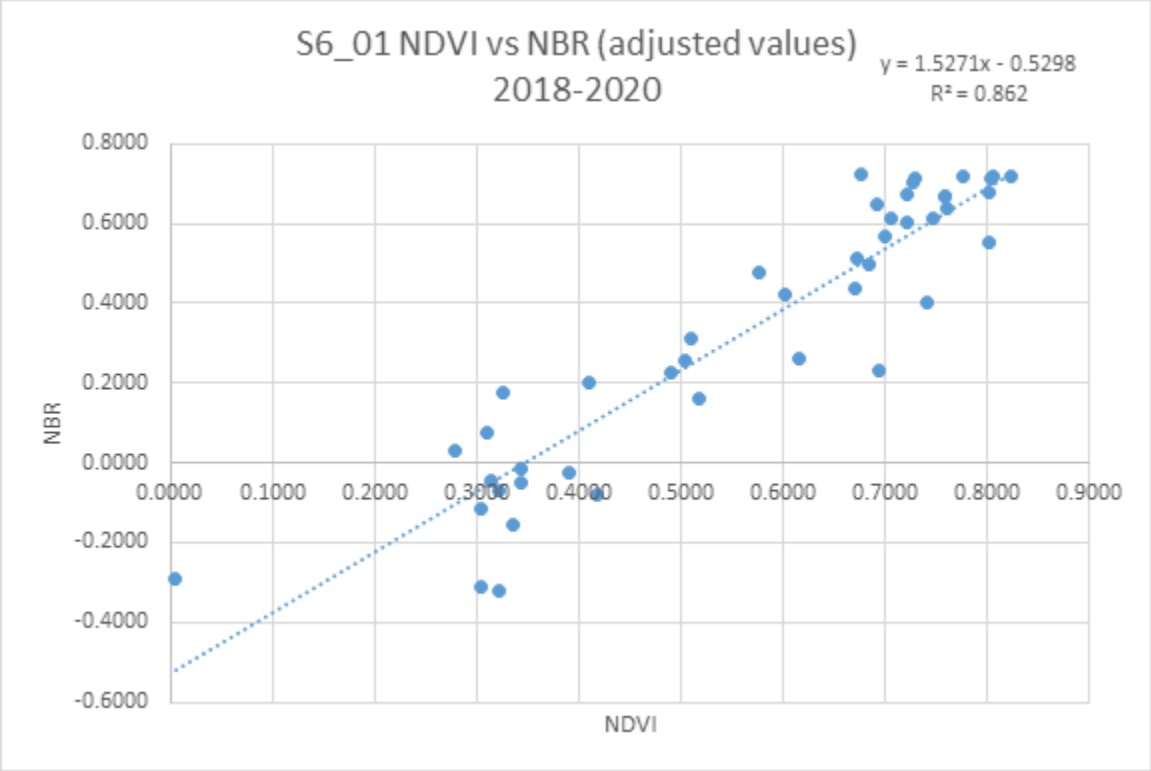

Figure 10. S6_01 NDVI vs NBR (adjusted values).

Graphical comparison of NDVI and NBR following data adjusting. After excluding the unusable data, a total of 45 data points from 2018 to 2020 were used. The R^2 value of 0.862 shows very strong correlation between the variables.

I then ran a time-series of the NDVI and NBR. Data points from 2018- 2020 were limited and resulted in multiple gaps in the curves. The missing data were attributed to cloud cover, as previously illustrated in Table 4. The three curves generally follow the sugarcane seasonal production, with the exception of the orange data set, EAA_NE_02 (Figure 11). Further inspection of this location indicated this field appeared to be fallow in 2019. Due to the limited amount of data, it was difficult to determine any trends; additionally, it was not possible to identify anomalies. Therefore, additional data was needed to continue my analysis.

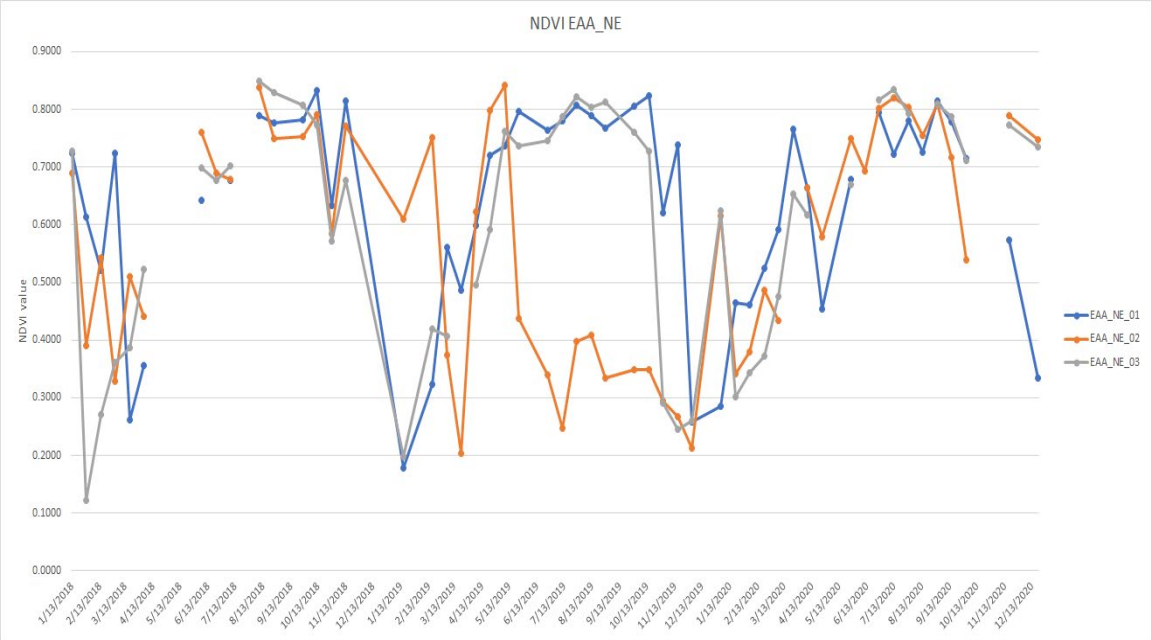

Figure 11. NDVI EAA_NE time series graph.

Time-series of NDVI from 2018 to 2020 using the manually correct data. Data includes the three SPs in the northeast section of the study area.

The purpose of this lengthy exploration phase was to familiarize myself with the general patterns and potential anomalies of the data. This phase was also carefully managed and calculated to ensure I understood what was occurring within my study area. Once I was certain about the patterns, anomalies, and statistical correlations, I wanted to expand the time-frame to further explore the anomalies in the data. Processing three years was very time consuming, and to expand my data set to twenty years, an alternative source was needed. This method needed to have a way of automating the calculations using cloud computing resources, and address cloud interference. I needed to utilize data that were preprocessed and mitigated cloud interference via masking. These data could be derived from Climate Engine (Climate Engine, 2022).

Climate Engine Data

The Climate Engine database is an extensive resource that provides LandSat imagery in a different format than the USGS EarthExplorer database. Climate Engine utilizes LandSat and other sourced data images that have been processed for surface reflectance and masked to removed cloud interference, and then calculates NDVI. Climate Engine does not provide the preprocessed images, but rather provides the processed images for a selected region derived from the Google Earth Engine. The processed map image is available to download, but only as a PDF.

The Climate Engine website describes the cursory process to remove interference from atmospheric conditions:

> Climate Engine applies a cloud mask to the Landsat TOA/SR (top of atmosphere/surface reflectance) data. The cloud masking attempts to remove medium and high confidence snow, shadow and cirrus clouds using the BQA quality band provided in the Landsat GEE collection (Climate Engine, 2022).

Due to the calculated high statistical correlation between the NDVI and NBR values at each SP (Figure 8), I was able to utilize only the Climate Engine NDVI values and know with high confidence NBR would follow the same pattern as NDVI. The initial time-consuming manual calculation then statistically justified the use of a semi-automated Climate Engine images to incorporate additional data over a much longer time span, 20 years.

The first step was to select which remote sensing dataset I wanted the data supplied from. Since I wanted a 20-year span and the range to include the time span I manually processed, the date ranged from January 1, 2000 to December 31, 2020. This date range encompasses multiple LandSat satellites, LandSat 5, 7, and 8. I chose the option for Climate Engine to pull data from all three satellites rather than individual

satellites. This allowed for a more seamless and consistent dataset of my specified time range.

After the data selection process, I had to define where I wanted Climate Engine to calculate the NDVI values from. I selected a small area, approximately ten by two (10×2) meters, in three regions adjacent to ground stations (G325, G434, and S6) with substantial nitrogen data. Climate Engine calculated the average NDVI for the entire drawn polygon. I drew specific polygons to only include vegetation pixels and not be near any roads, structures, or canals. This minimized, ideally eliminated, the inclusion of erroneous NDVI values. The polygons were a much closer representation of the study points selected during the exploratory phase. The returned data (averaged NDVI per polygon) from Climate Engine was provided as a comma separated value (CSV) file.

The Excel data only provided the date and corresponding NDVI value for the entire LandSat 5 to 8 range, i.e., March 24, 1984 to March 29, 2022 (present day at the time of download). The data sets needed to be reduced to only include the 20-year time range, as specified above. The next steps were to perform statistical analyses and graphing to make sense of each data set and analyze the Climate Engine data against the ground station data.

Statistical Calculations

To account for the variation in the NDVI, the data were standardized, also referred to as Z-score or mean centering. The purpose of standardizing the data is to allow direct comparison of data that couldn't normally be compare together, e.g.,

precipitation and NDVI, due to the unit, range, and/or scale disparities. All of the Climate Engine 2000-2020 data points were processed using the following formula:

$$Z_X = \frac{(X - \mu)}{\sigma}$$

where:

- Z_X is the newly calculated z-score for a data point
- X is the data point
- μ is the mean value of the 2000-2020 data
- σ is the standard deviation of the 2000-2020 data

In addition to NDVI, I standardized the Nitrate+Nitrite-N (Nitrogen) data. As described previously, Nitrate+Nitrite-N is the most common and continuous test performed, as seen in Table 3, to monitor water quality for nitrogen problems (excluding organic nitrogen and ammonia). This nitrogen test would show if nitrogen loss was occurring from cultivated sugarcane land. The calculated Z-scores were then plotted as a time-series from 2000 to 2020 (Figure 12). The large degree of fluctuation in NDVI was due to the sugarcane growth/harvest cycle, which can be easily seen annually. The nitrogen fluctuation is less consistent in seasonality, but the peaks do occur during the late spring and summer months.

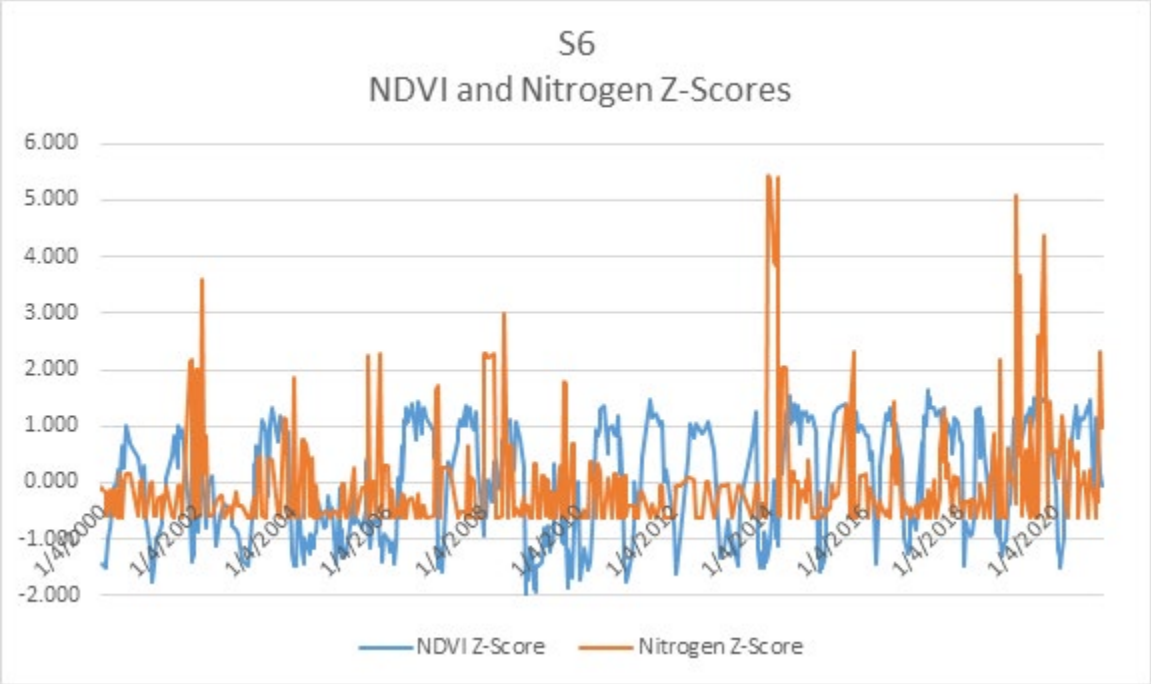

Figure 12. S6 NDVI and nitrogen Z-scores.

Z-score time-series of NDVI and nitrogen values at the S6 ground station location. Due to large amount of fluctuation between the two variables, this graph is difficult to interpret.

Because a pattern was difficult to determine from this graph (Figure 12), another approach was taken, calculating a statistical outlier. An outlier was determined by using the following formula in Excel:

$$= IF(X > 3,1,0)$$

where:

- X is the cell value
- 3 is the standard deviation
- 1 and 0 are the outputs. 1 if true. 0 if false.

The outlier was determined by utilizing a typically used standard deviation value of 3; a standard deviation of 3 indicates a data point value must be above 99.7% to be determined as an anomaly. The standard deviation value can be reduced, typically only down to 2.5, to increase sensitivity of the anomaly calculation.

An alternate value was used in the formula for the NDVI outlier determination. The cell value, i.e., NDVI value, had to be < -0.99 to report an anomaly. The value of -0.99 was determined based on the NDVI upper limit of the previously determined burned ground during the supervised thresholding (Table 6), below an empirically derived NDVI value of 0.35. Then 0.35 was subtracted from the mean value of the NDVI data and the result was then divided by the standard deviation of the NDVI data set.

$$NDVI\ anomaly\ threshold = \frac{(\mu - 0.35)}{\sigma}$$

where:

- μ is the mean value of the NDVI data set
- 0.35 is the predetermined NDVI upper limit of burned ground
- σ is the standard deviation of the NDVI data set

I performed the calculations with the precipitation data based on a variation of the outlier equation above. I wanted to include multi-day (up to 3 days) rain events. When the data were based on individual days it would not have met the outlier criteria in many circumstances, but the sum of the multi-day event met the criteria to classified as an anomaly. The equation below illustrates the summation of the day before, day of, and day after, with clauses to eliminate over estimation of anomalies.

$$= IF(X_{day(n)} > 2.5,1, IF\left(\sum\left(IF(X_{day(n-1)} < 2.5, X_{day(n-1)}, 0\right)\right.\right.$$

$$+ IF\left(X_{day(n)} < 2.5, X_{day(n)}, 0\right) + IF(X_{day(n+1)} < 2.5, X_{day(n+1)}, 0\Big)$$

$$> 2.5,1,0)$$

where:

- $X_{day(n)}$ is the cell value on a selected day
- $X_{day(n-1)}$ is the cell value on the day before the selected day
- $X_{day(n+1)}$ is the cell value on the day after the selected day
- 2.5 is the standard deviation
- 1 and 0 are the outputs. 1 if true. 0 if false.

The precipitation formula threshold for an anomaly was also reduced to 2.5. The purpose of reducing the standard deviation was to increase the sensitivity of the calculations. Erosion does not only need an anomalously large volume of water over a short time to cause soil erosion. Rather, erosion can still occur with a large enough volume of water over an extended period of time, which I calculated as anomalies using precipitation over three days.

The nitrogen data anomalies were calculated similarly to the precipitation data, but the threshold was reverted back to 3. An increase in sensitivity was not needed for this variable.

Once the anomalies were determined for the three variables, I plotted the anomalies on a time-series (Figures 13-16). It is difficult to discern any notable pattern for these graphs that span 20 years . This is mainly due to the large amount of

precipitation data. But even when precipitation was removed, the graph was too difficult to interpret. The difficulty appeared to be based on the too large of scale.

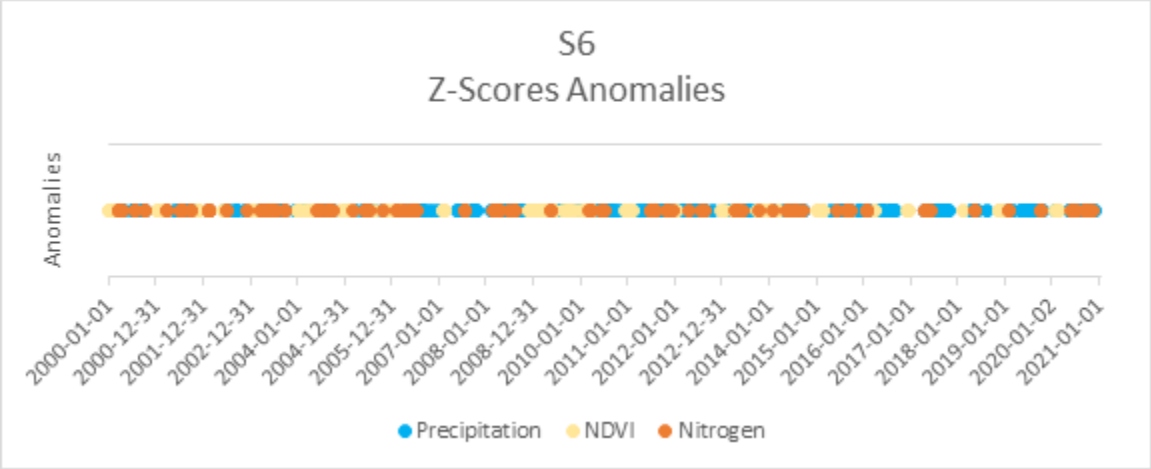

Figure 13. S6 Z-scores anomalies (precipitation, NDVI, & nitrogen).

All three variables shown. This graph is difficult to interpret due to the overlapping data points.

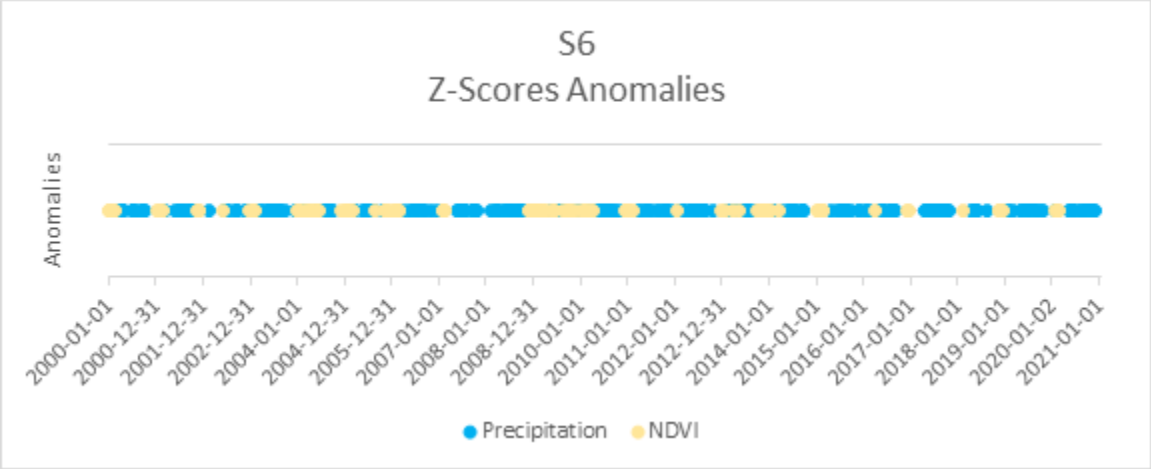

Figure 14. S6 Z-score anomalies (precipitation & NDVI).

Only NDVI and precipitation anomalies shown. The graph is still just as difficult to interpret due to the overlapping large number of precipitation data points.

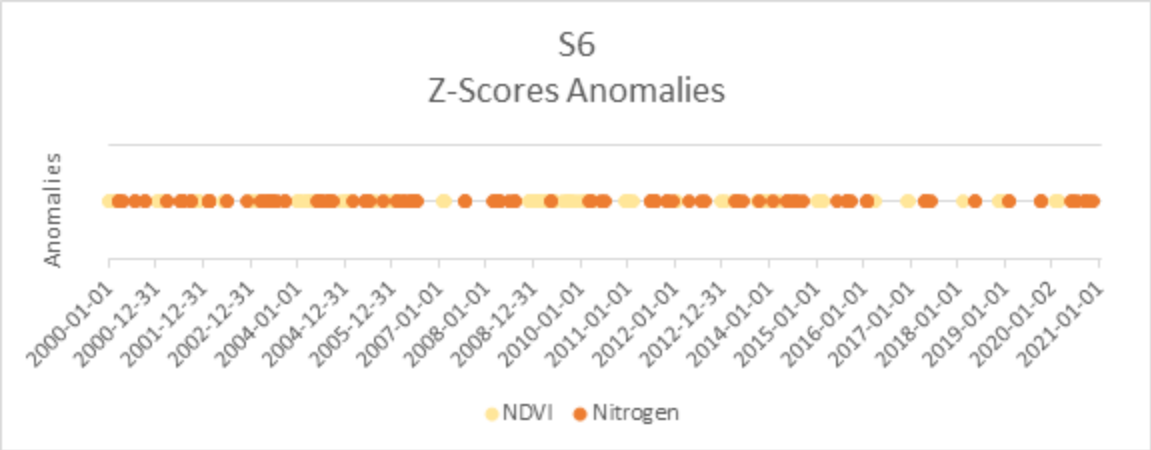

Figure 15. S6 Z-score anomalies (NDVI & nitrogen).

Only NDVI and nitrogen anomalies shown. This graph is still difficult to discern a notable pattern due to the overlapping data points, but some clustering can be observed.

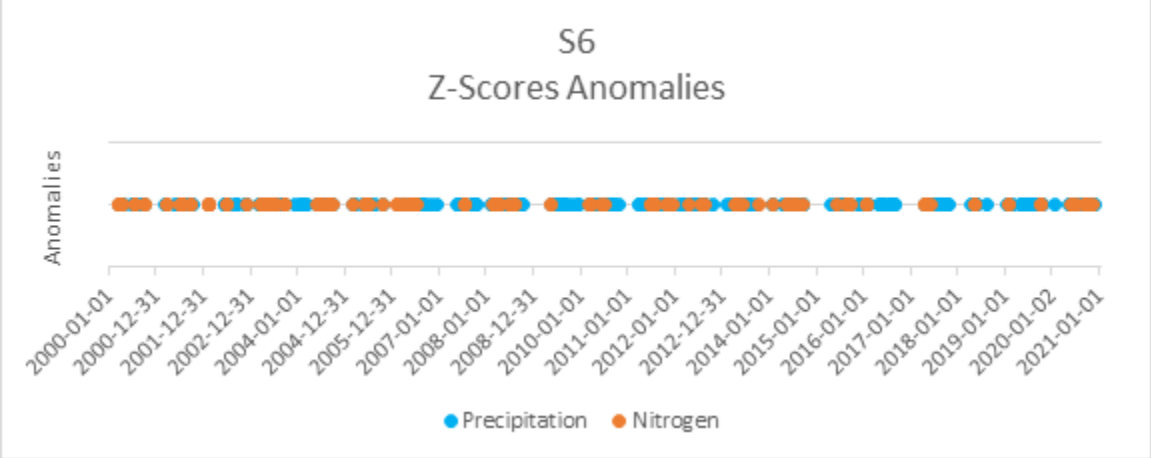

Figure 16. S6 Z-scores anomalies (precipitation & nitrogen).

Only nitrogen and precipitation anomalies shown. This graph is also too difficult to read due to the large number of overlapping precipitation data points.

To address this, I zoomed in to focus on smaller segments that covered only a few years at a time, 2014 to 2018 (Figure 17). I also wanted to directly compare the three

regions' anomalies by juxtaposing them on a single graph. Clustering is observed for all three variables on a yearly basis (Figure 17).

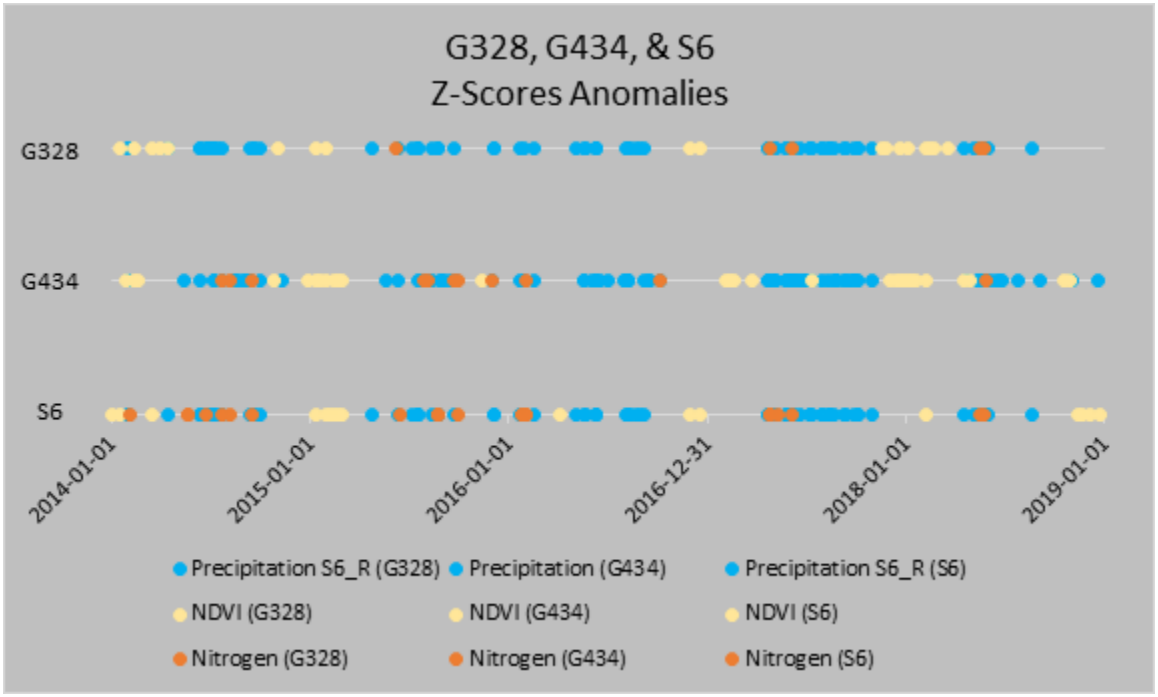

Figure 17. G328, G434, & S6 Z-scores anomalies

Nitrogen, NDVI, and precipitation anomalies shown for the G328, G434, and S6 ground station regions.

Once the statistical analyses and interpretation were complete, I was able to move on to the final segment, a cost benefit analysis of suggested options for mitigation of the potential impacts described above.

Cost Benefit Analysis

To provide the sugarcane industry a viable alternative to burning sugarcane, I wanted to present multiple options for sustaining this agricultural business. I sourced a

prebuilt sugarcane cost-benefit analysis (CBA) model from the Louisiana State University (LSU) Agriculture Center (Deliberto & Hilbun, 2019). The LSU CBA model is very thorough and I was able to eliminate multiple unneeded sections (e.g., weighted average calculator for mill share for sugarcane). I also did not include costing of equipment.

Model Inputs

The inputs chosen for the CBA were based on published sugarcane research through the University of Florida IFAS Extension (UF/IFAS) (McCray et al. 2019; McCray, Morgan, & Baucum 2019; Rott et al. 2018). I chose the 2018-2019 season due to more readily available data. The initial inputs were: how much sugarcane per acre was produced and how much sugar was extracted per tons of sugarcane. Both variables were dependent on the variety of sugarcane. UF/IFAS reported (UF/IFAS 2019) variety CP 96-1252 (CP96) was most prevalent during the 2018-2019 season. The reported values for CP96 were dependent on soil type: 57.1 tons/acre in sand to 48.9 tons/acre in muck (peat), 329.4 sugar/ton in sand and 287.2 sugar/ton in muck. I assumed 50% sand and 50% muck, resulting in 53 tons/acre and 308 sugar/ton. A more accurate distribution of the soil type in the study area could have been done, but would likely not be accurate for 2019, only 2022.

To simplify the model, multiple ratoons were not taken into account due to the sugar data not being available. Instead, the data was repeated for up to three ratoons. The total acres of land, within my study area, was approximately 93,292 acres. I assumed that approximately 80% of the land was cultivated for sugarcane. I adjusted land use values accordingly throughout, keeping the same percentages as the original

LSU model. The remaining costs I left unchanged. These costs ultimately do not play a role in the proposed sustainable options.

After completing the baseline CBA model, I adjusted the model to reflect three proposed sustainability options:

1) Replace old sugarcane harvesters with updated models able to harvest unburned sugarcane. The harvesters are also able to sort the green trash from the sugarcane, which can be left behind or containerized.

2) Process the bagasse and green trash into biochar, which is a solid carbon material produced from pyrolysis of an organic material (in this case, sugarcane). The biochar can then be sold to agricultural businesses as a soil supplement.

3) Use cover crops during fallowed field cycles, i.e., every fourth year, to help stabilize the soil and act as a soil regenerative practice.

The first sustainability option, replacing the harvesters with updated models, was based on the John Deere CH570 sugarcane harvester. This particular model was a more middle of the road priced machine, $605,000, and had the engineering improvements for a sustainability/cost-benefit analysis model: 20% labor cost reduction due to efficiency, 20% harvest time reduction due to the improve machinery, and a potential 15% increase in the quality of the sugarcane; i.e., an increase in the sugar per ton, due to the redesigned cutting/harvesting mechanisms (note: all of these percentages are approximations that were provided by John Deere). I adjusted the CBA model accordingly to reflect the reductions and increases in variable values (Figures 18 & 19, respectively).

Harvest - 2-Row Wholestalk Harvester				
Expense Item	**Unit**	**Price**	**Quantity**	**Cost**
Labor	acre			21.14
Fuel - Tractors	gal	$2.50	9.07	18.14
Fuel - Wholestalk Harvester	gal	$2.50	6.38	12.76
Repair & Maintenance	acre			37.57
Other	acre			0.00
Other	acre			0.00
Other	acre			0.00
Interest on Oper. Capital	acre			5.65
Projected Wholestalk Harvest Expenses				**$95.27**

Figure 18. Harvester CBA Model – harvester expenses.

The cost per acre for harvesting sugarcane after a 20% decrease in Labor, Fuel – Tractors, and Fuel – Wholestalk Harvester. The baseline value for labor was $26.42/acre, Fuel – Tractor was $22.68/acre, and Fuel – Harvester was $15.95/acre.

Projected Whole Farm Sugarcane Costs and Returns for the 2019 Crop Year									
Total Farm Acres	93,292.0			Dollars Per Acre	Number of Acres	Total Dollar Value	Dollar Value Per Acre	Value Per Pound of Sugar
Total Acres Harvested for Sugar	75,000.0							
Raw Sugar Price per Pound	$0.191							
Molasses Price per Gallon	$0.55							
Total Sugarcane Production (tons) =			**3,975,000**					
Total Raw Sugar Production (lbs) =			**1,407,945,000**	*($/acre)*	*(acre)*	*($)*	*($/acre)*	*($/lb of sugar)*
Gross Value of Production:								
Sugar:	tons/acre	sugar/ton	sugar/acre					
Plant Cane	53.0	354	18,773	3,579.93	18,750.0	67,123,778	719.50	0.191
1st Stubble	53.0	354	18,773	3,579.93	18,750.0	67,123,778	719.50	0.191
2nd Stubble	53.0	354	18,773	3,579.93	18,750.0	67,123,778	719.50	0.191
3rd Stubble	53.0	354	18,773	3,579.93	18,750.0	67,123,778	719.50	0.191
Older Stubble	0.0	0	0	0.00	0.0	0	0.00	0.000
					75,000.0			
Total Market Value of Sugar Production						**$268,495,112**	**$2,878.01**	**$0.191**
Molasses: Gal. Mol./Cwt. Sugar			3.0					
Gallons of Molasses			42,238,350	--	--	**$23,231,093**	**$249.01**	**$0.017**
Total Market Value of Sugar & Molasses						**$291,726,204**	**$3,127.02**	**$0.207**

Figure 19. Harvester CBA Model – projected values.

Projected sugarcane production value after adjusting for a 15% increase in sugar/ton produced. The baseline value was 308 sugar/ton.

The second sustainability option was to utilize the green trash and bagasse to produce biochar. I assumed that only 75% of the fields were currently active each year

and 25% of the fields were fallowed. Once the weight, in tons, per acre was calculated, I utilized the typical price and production rates of a biochar machine. The amount of biochar produced is approximately 10% the total weight supplied. The next calculation was to determine how much weight could be converted within a 90-day window, the approximate time sugarcane green trash and bagasse can be used before degradation (Bhadha et al., 2020). The total biochar produced would be 19,440 tons. To utilize all of the green trash and bagasse available, it would take approximately 189 days, with thirty (30) machines running 24 hour per day. Since this was passed the 90 days, the leftover green trash, approximately 215,322 tons would be utilized as ground cover. The biochar gross cost and production costs were calculated. Then the total net production cost of the biochar could be calculated. The operational costs, purchase price of the ten biochar machines, and gross income were added to the CBA model. Figure 20 illustrates the full calculations of the biochar production.

Green trash	
12.5	Green trash per hetare (metric tons)
34.0	**Tons per acre**
15%	total above ground biomass
75%	left behind
Bagasse	
140	kg per 1 metric ton of sugarcane
308.6	lb per 1 metric ton
340.2	lb per 1 ton
18,032	lbs per acre
0.14	metric tons per 1 metric ton of sugarcane
0.15	tons per 1 ton
8.2	**Bagasse per acre (tons)**
Biochar	
$250,000	Purchase price per machine
3	Rate (tons/hour)
90%	Eliminates waste material
72	Power needed (kW/hour)
$139.00	Power cost per hour

0.3	Biochar production rate (tons/hour)
$1,714.29	Biochar price ($USD per ton)
	Production
1,915,221	Total green trash (tons)
460,077	Total of bagasse (tons)
75%	Loss of bagasse to power plants
115,019	Net bagasse (tons)
2,030,240	**Total green trash & bagasse (tons)**
90%	Green trash left in place
255,363	Total green trash (tons)
153,359	Total bagasse (tons)
408,722	**Total green trash & bagasse (tons)**
30	Number of biochar machines
4,541	Total hours needed to convert everything
189	Total days needed
19,440	Biochar produced (tons)
214,322	Leftover biomass (tons)
$33,325,714	**Gross total of biochar produced**
$7,500,000	Purchase price of biochar machines
$9,007,200	Fuel cost to run biochar machines
$10,252,740	Other operational costs for biochar machines
$19,259,940	**Total Costs**
$14,065,774	**Net Returns for Biochar**

Figure 20. Biochar CBA Model – biochar production costs.

Biochar production cost-benefit calculations. The Gross total of biochar, Fuel cost, and Other operational costs were plugged into the CBA model for sustainability option 2.

The third sustainability option was to use cover crops, in particular Sunn Hemp, during the fallowed fourth year for each field. The total amount of seed needed for 18,750 acres was 750,000 pounds of seeds. The cost of Sunn Hemp seed was $1.40 per pound with the total price of seeds $1,050,000. The Sunn Hemp would be plowed back into the field prior to replanting. The benefits gained from utilizing Sunn Hemp as a

cover crop was an approximate 33% reduction in fertilizer costs and 20% reduction in pest control. These two reductions were directly plugged into the Field Operations costs. The associated costs of planting a cover crop were calculated to be $56 per acre. Figure 21 illustrates the CBA costs per acre of the Sunn Hemp fallow option. Figure 22 shows the forecasted savings in fertilizer and insecticides for sugar cane production by fallowing with Sunn Hemp,

Fallow Expenses (including plowing old stubble, seedbed prep)				
Expense Item	**Unit**	**Price**	**Quantity**	**Cost**
Herbicides	acre			14.70
Labor	acre			29.69
Fuel	gal	$2.50	21.88	54.70
Repair & Maintenance	acre			22.69
Service Fees	acre			7.00
Sunn Hemp Seeds (per pound)	acre	$1.40	750,000	56.00
Other	acre			0.00
Other	acre			0.00
Interest on Oper. Capital	acre			3.80
Projected Fallow Expenses				**$188.58**

Figure 21. Cover Crop CBA Model – Sunn Hemp expenses.

Cost of Sunn Hemp seeds per pound and calculated cost per acre.

Plant Cane Cultivation and Field Operations					
Expense Item		**Unit**	**Price**	**Quantity**	**Cost**
Custom Aerial Appl.		appl.	$4.00	2	8.00
Fertilizer - Nitrogen		lbs of N	$0.43	0	0.00
Fertilizer - Phosphorus		lbs of P	$0.55	54	29.48
Fertilizer - Potassium		lbs of K	$0.32	54	17.15
Fertilizer - Other	Other	lbs	$0.00	0	0.00
Herbicides		acre			74.63
Insecticides		acre			23.81
Service Fees		acre			7.00
Labor		acre			17.89
Fuel		gal	$2.50	11.33	28.33
Repair & Maintenance		acre			10.84
Surfactant		acre			5.60
Other		acre			0.00
Other		acre			0.00
Interest on Oper. Capital		acre			6.92
Projected Plant Cane Cultivation Expenses					**$229.65**

Figure 22. Cover Crop CBA Model – reductions of expenses.

The 33% reduced quantities of fertilizer due to the use of Sunn Hemp. The baseline had quantities at 80 pounds for the plant cane cultivation. The first, second, and third stubbles had increased quantities, 100 pounds, that were reduced to 67 pounds.

Following analyses of the baseline and three sustainability options, I performed a comparison of the net returns for the four scenarios. Using CBA, I was able to compare the total dollar value, dollar value per acre, and the value per pound of sugar. The purpose was to determine if any of the sustainable options were profitable, providing a viable alternative to burning, thus addressing my second hypothesis.

Chapter III

Results

The results will be discussed in light of my two research questions and their associated hypotheses:

1. What is the relationship between the traditional sugarcane practice of pre-harvest burning and nitrogen levels in nearby wetlands?
    - H1a: I anticipated there is a direct correlation between the sugarcane field burning within the EAA and increased nitrogen, with precipitation as a driving transport mechanism, within the downgradient water.
    - H1b: I expected to see regional differences between the scale of the burning each year and the environmental impact, i.e., soil loss as measured by nitrogen in the water.
2. Can a sustainable change be made to the traditional field burning practice that will allow for future economic growth of the commercial sugarcane industry?
    - H2a: I expected that substantial environmental benefits can be realized by mitigating N impacts by altering sugarcane farming practices to reduce burning.
    - H2b: I expected some of the alternative practices to burning to be cost-effective.

The results are presented in the form of: 1) ground station data and its analyses; 2) satellite data and its analyses; 3) the initial LandSat based Climate Engine and statistical time series; and 4) a comparison of the cost benefit analyses.

Ground Station Data

The graphs for each ground station show a general yearly seasonality of the nitrogen data (Figure 23); these are for Nitrate+Nitrite-N (N+N), which stands for the chemical analysis of nitrate compounds plus nitrite compounds as nitrogen (N), for each ground station. The ground station data adjacent to my study area were limited to only the canals at the southern end of the study area. The ground station S2, located at the edge of Lake Okeechobee, was selected to serve as the upgradient point. The ground station S7, located downgradient, was selected as due to two major canals intersecting at this location. The three study area ground stations and up- and downgradient ground stations are shown on Figure 7.

The high density of data in these graphs made it difficult to clearly interpret a specific trend due to the variability in the data. To address this, a trendline of a 20% moving average was added to each graph to more clearly illustrate the trend (Figure 23). A trendline of 20% was chosen after examining 5%, 10%, and 15% and determining 20% illustrated the general trend of the data without losing too much of the curvature of the seasonality. This moving average illustrates the trend with less sensitivity to outlying data points, i.e., the elevated points are taken on average not a singularity. Thus, cleaner, more easily interpreted graphs were produced showing a more obvious seasonality trend of the nitrogen data.

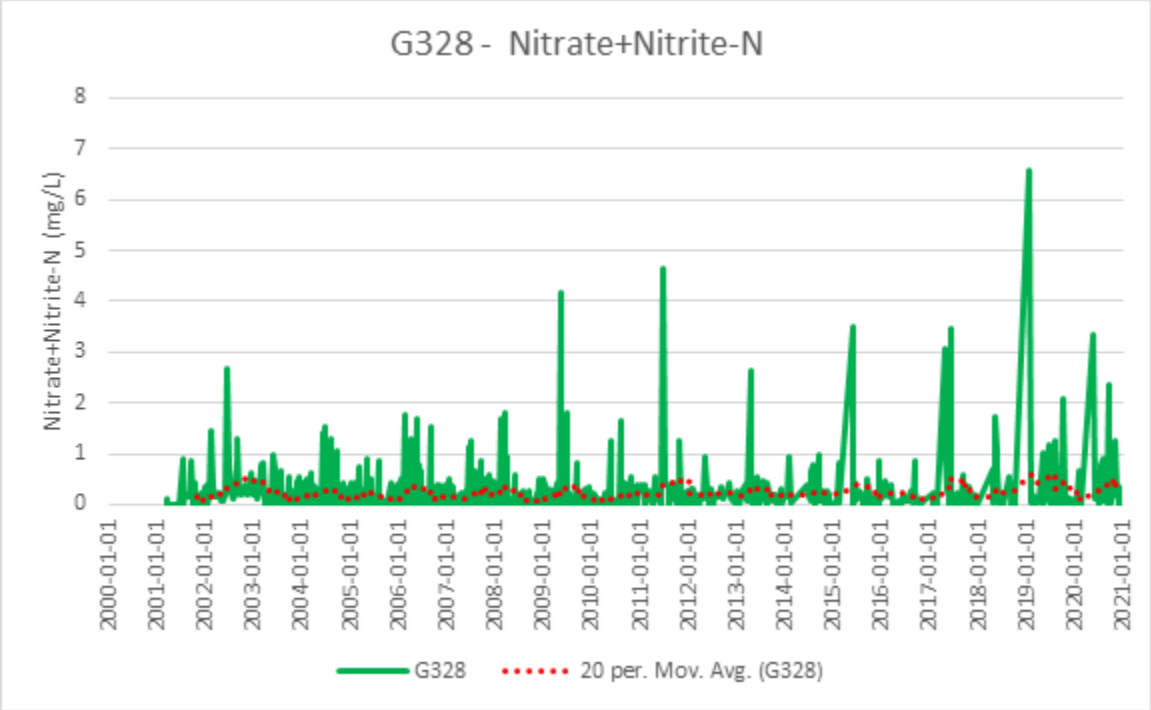
G328 - Nitrate+Nitrite-N
Nitrate+Nitrite-N (mg/L)
0
1
2
3
4
5
6
7
8
2000-01-01
2001-01-01
2002-01-01
2003-01-01
2004-01-01
2005-01-01
2006-01-01
2007-01-01
2008-01-01
2009-01-01
2010-01-01
2011-01-01
2012-01-01
2013-01-01
2014-01-01
2015-01-01
2016-01-01
2017-01-01
2018-01-01
2019-01-01
2020-01-01
2021-01-01
G328
20 per. Mov. Avg. (G328)

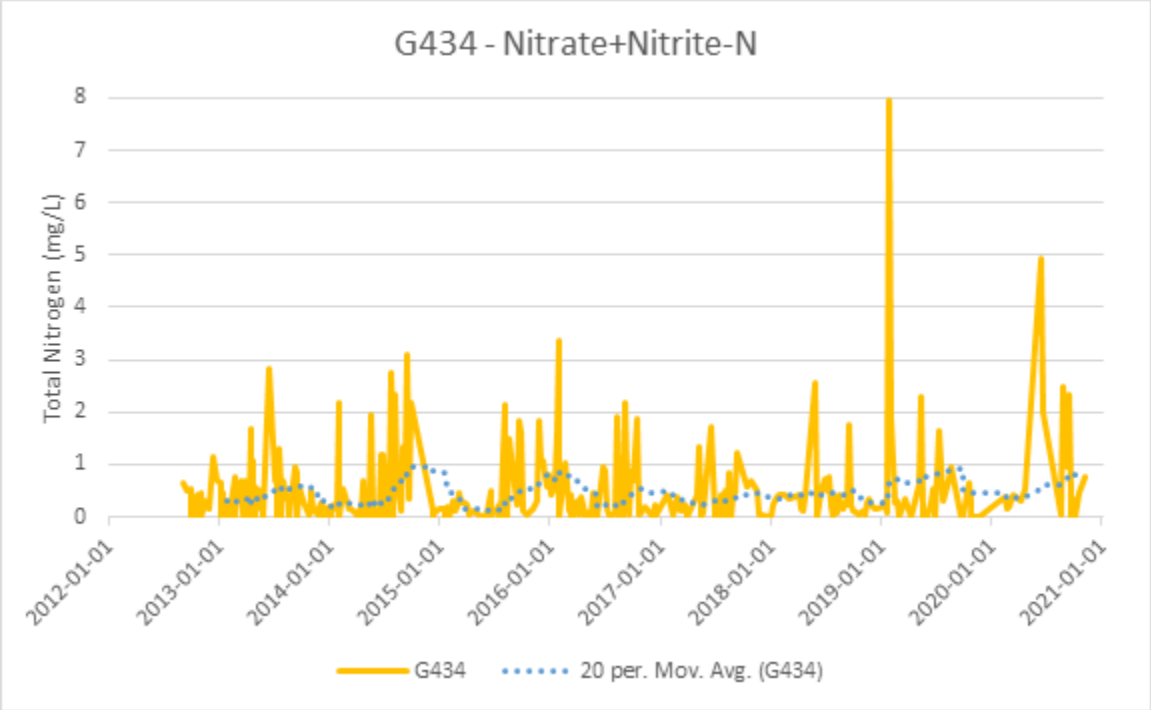
G434 - Nitrate+Nitrite-N
Total Nitrogen (mg/L)
0
1
2
3
4
5
6
7
8
2012-01-01
2013-01-01
2014-01-01
2015-01-01
2016-01-01
2017-01-01
2018-01-01
2019-01-01
2020-01-01
2021-01-01
G434
20 per. Mov. Avg. (G434)

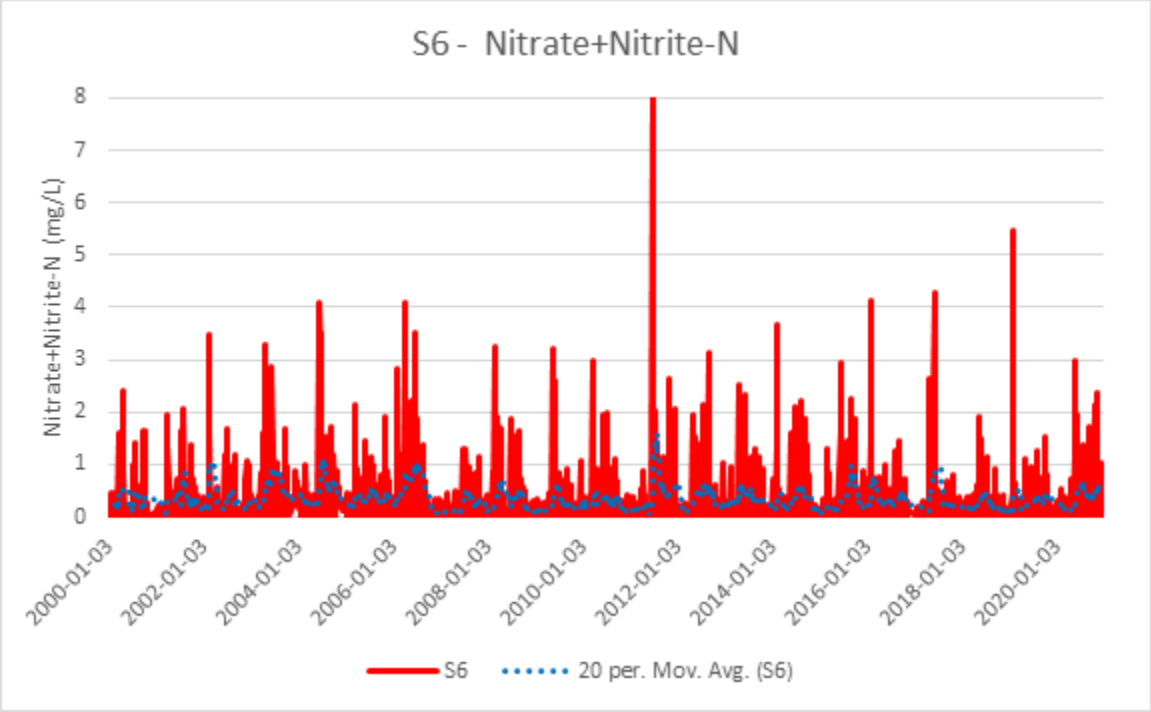
S6 - Nitrate+Nitrite-N
Nitrate+Nitrite-N (mg/L)
0
1
2
3
4
5
6
7
8
2000-01-03
2002-01-03
2004-01-03
2006-01-03
2008-01-03
2010-01-03
2012-01-03
2014-01-03
2016-01-03
2018-01-03
2020-01-03
S6
20 per. Mov. Avg. (S6)

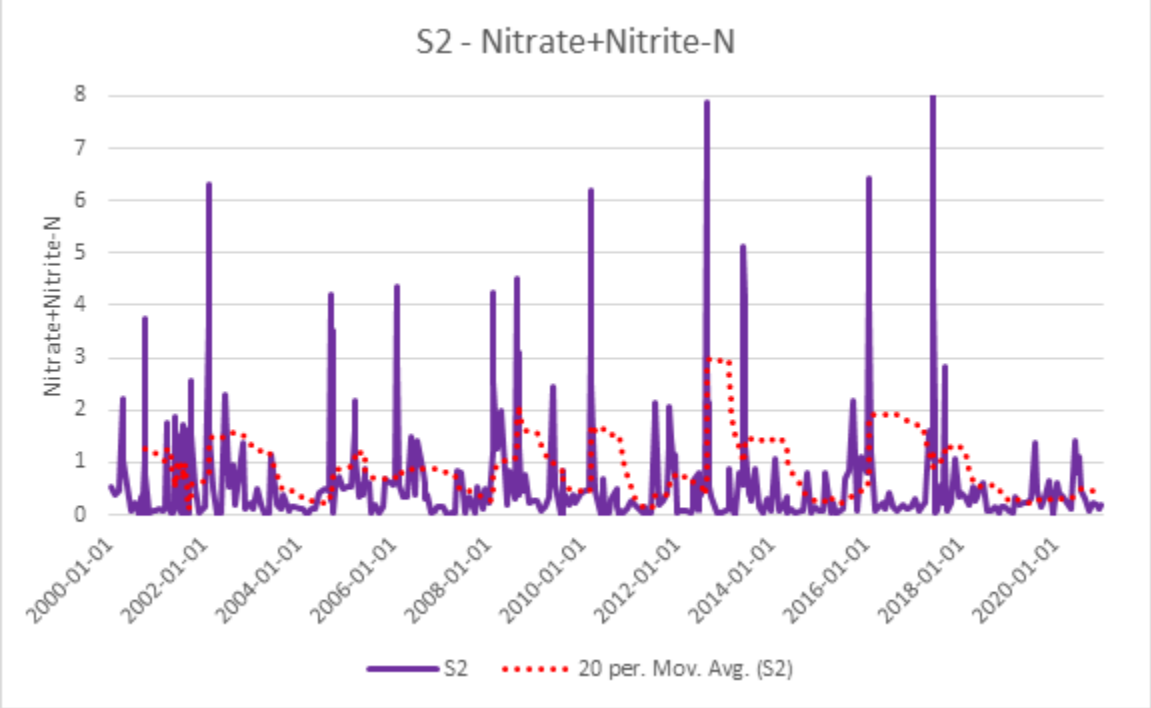
S2 - Nitrate+Nitrite-N
Nitrate+Nitrite-N
0
1
2
3
4
5
6
7
8
2000-01-01
2002-01-01
2004-01-01
2006-01-01
2008-01-01
2010-01-01
2012-01-01
2014-01-01
2016-01-01
2018-01-01
2020-01-01
S2
20 per. Mov. Avg. (S2)

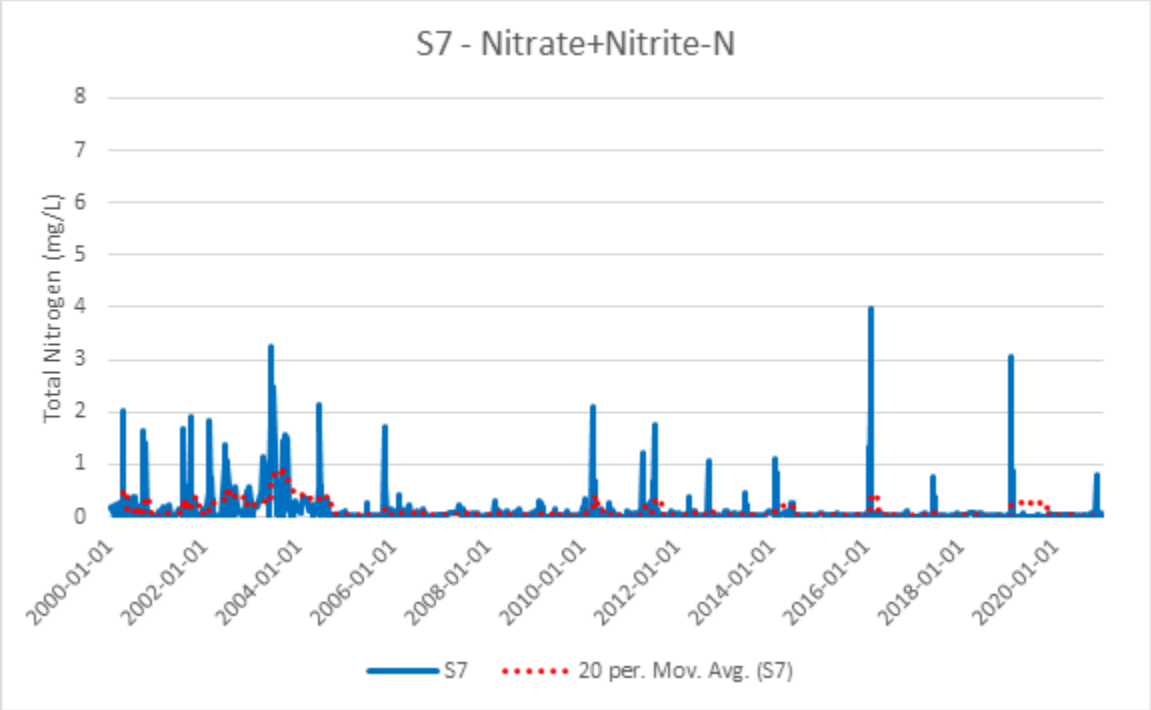

Figure 23. Water nitrogen concentration for the G328, G434, S2, S6, & S7 ground stations, 2000-2020.

Nitrate+Nitrite-N data from the G328, G434, S2, S6, and S7 ground stations. Data ranged from January 2000 to December 2020 at the study area ground stations (G328, G434, and S6) and up/down gradient ground stations (S2, upgradient, and S7, downgradient). Note that data collection began in 2001 and 2012 for G328 and G434, respectively. The trendline is a 20% moving average of the nitrogen data to illustrate the trend without being as influenced by outlying high values while still showing seasonal curvature.

To more clearly compare the nitrogen data from each ground station, graphs with three sets of data, as not to overcrowd the image, were produced, Figures 24 through 26.

Figure 24 has the ground stations located within the study area, G328, G434, and S6 (location presented on Figure 7). This graph shows the seasonal elevated levels of N+N at each ground station. It is notable that each ground station does not appear to illustrate the same pattern nor spikes in the data.

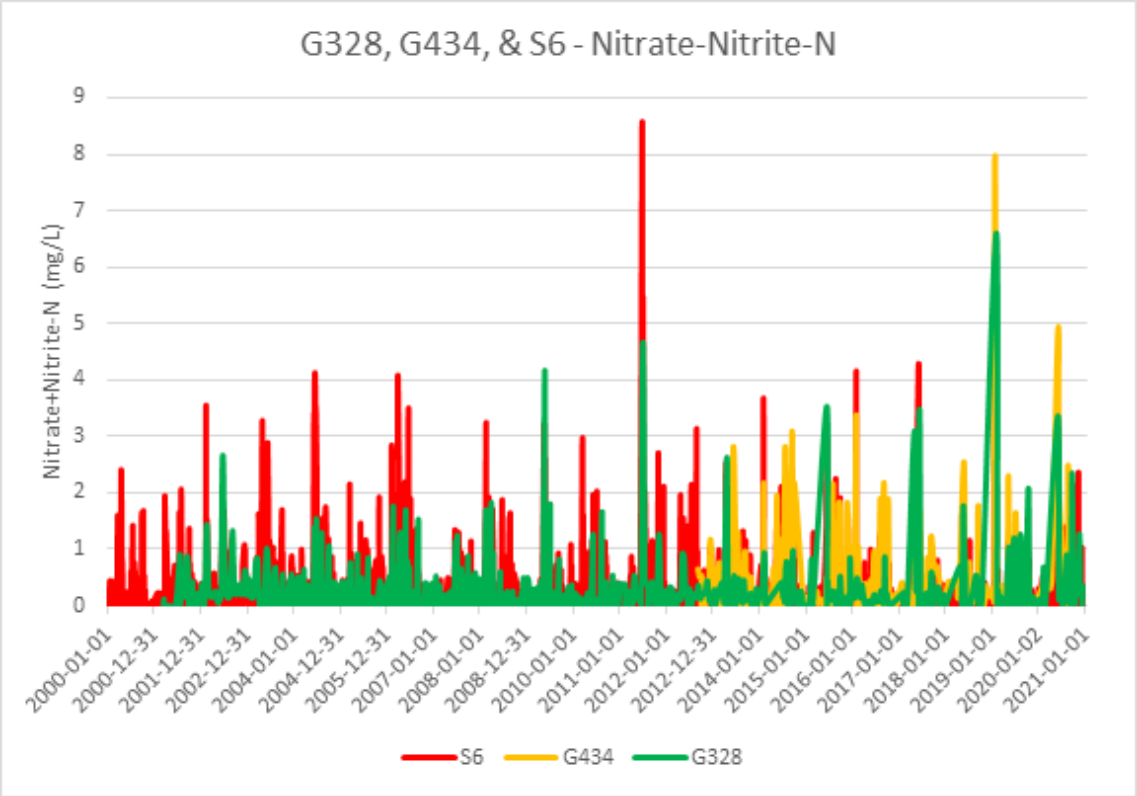

Figure 24. Nitrogen data from study area ground stations, G328, G434, and S6.

Figure 25 has two ground station within the study area, G434 and S6, along with the downgradient ground station S7. G434 was located on the western side of the study area and S6 was located on the east side. The S6 and S7 N+N levels from 2000 to early 2004 appeared similar in pattern and magnitude, but S7 had a drastic reduction in N+N levels from mid-2004 through 2020. This was likely due to mitigation efforts built by the SFWMD to reduce the nutrification within the Everglades, e.g., stormwater treatment areas (SWAs) and dispersion within the water while flowing downstream. In conclusion, the ground stations further away from the active sugarcane farming had reduced elevations of nitrogen in the water.

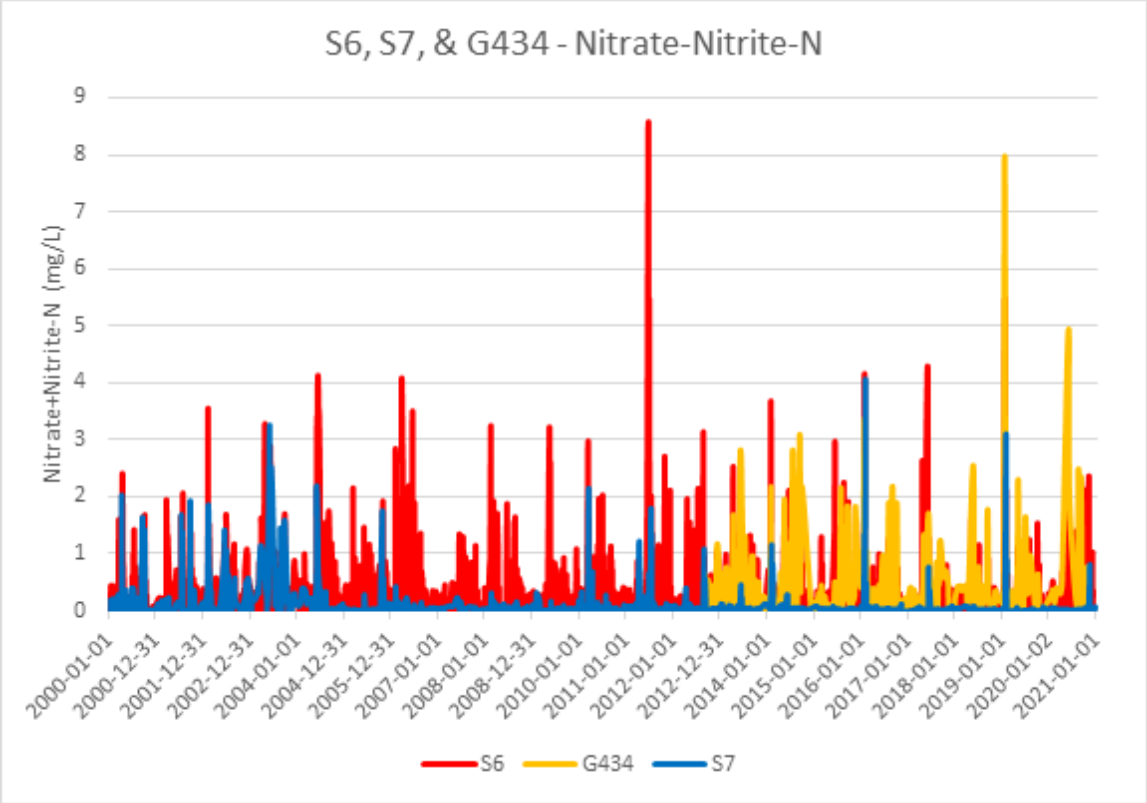

Figure 25. Nitrogen data from S6, S7, and G434 ground stations.

Figure 26 includes an upgradient, S2, and downgradient, S7, ground stations along with S6, which was located on the southeastern corner of my study area and on the edge of the EAA. This figure covers the furthest extent of analysis I performed. Figure 26 illustrates that the nitrogen levels found upgradient in Lake Okeechobee were elevated and remained so from 2000 through 2020. Additionally, the majority of S2 data above 4.5 mg/L had an analytical uncertainty of 50%. If this was not included (Figure 27), the nitrogen levels in S6 were more easily observed to be higher and do not match seasonally. The S6 nitrogen levels were typically higher than S2, except in 2012 and 2019. It's possible that due to high precipitation in 2012 and 2019, water was pumped from the EAA into Lake Okeechobee, resulting in increased nitrogen levels.

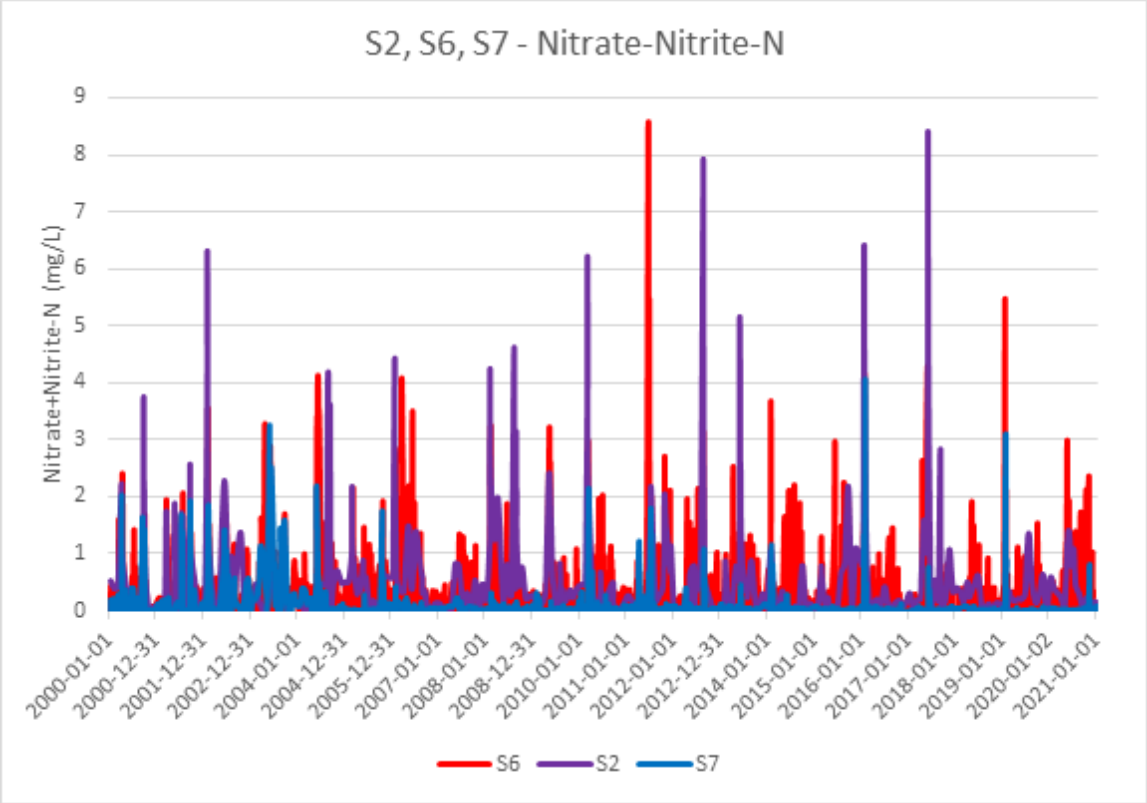

Figure 26. Nitrogen data from S2, S6, and S7, ground stations.

Data is shown from January 2000 to December 2020. S2 was upgradient outside of the EAA, S6 was on the southern end of the EAA, and S7 was down gradient of the EAA.

This higher N level in S6 compared to S2 indicates additional nitrogen is being introduced into the water from in-between, which is the EAA. As mentioned above, the S7 data was elevated compared to S2 and S6 until approximately early 2004, then remained on average lower through 2020 (Figure 26). Though mitigation efforts were being made to prevent elevated nitrogen concentrations from entering the Everglades, there was still a nitrogen source problem within the EAA, which predominately was occupied by sugarcane. The role of sugarcane will be explored utilizing satellite data in the next section.

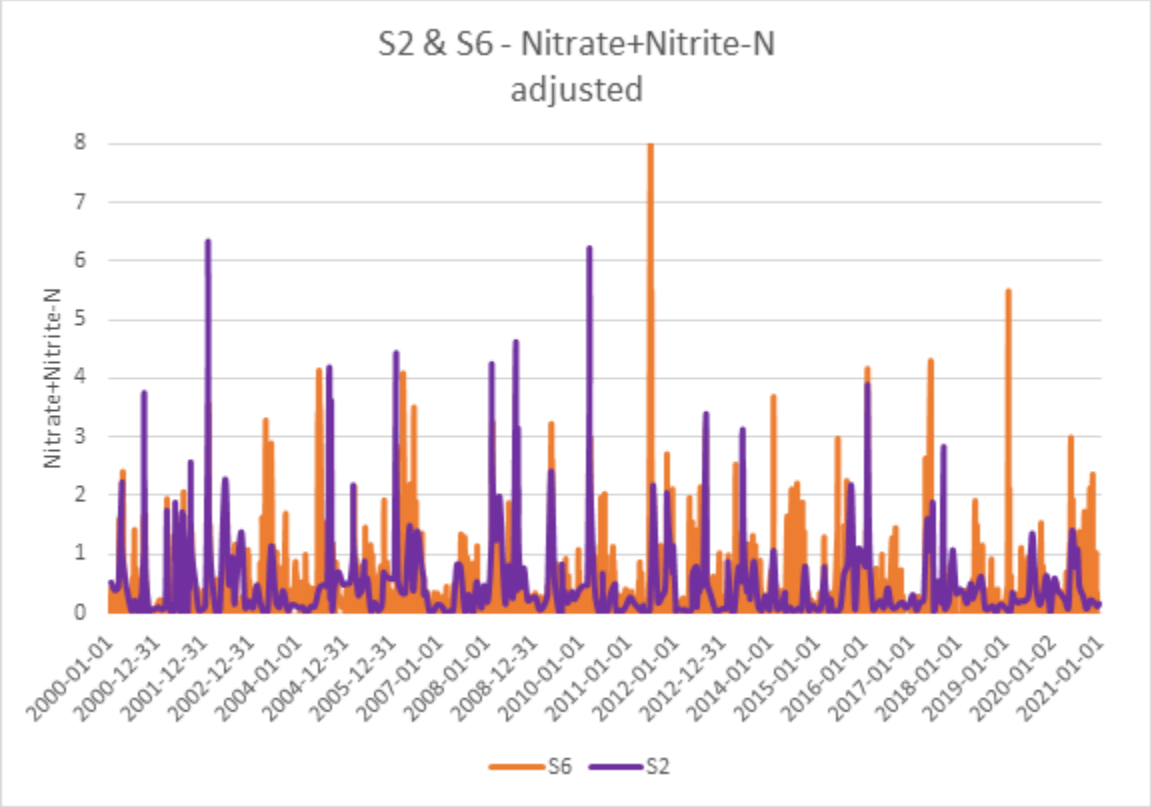

Figure 27. Nitrogen data from S2 and S6 ground stations.

Data from S2 has had the uncertain data removed.

Precipitation acts as a mechanism for soil erosion and transport from the sugarcane fields to the canals and subsequently downstream. In order to determine if the precipitation variable was vital to soil loss, and thus water nitrogen levels, precipitation data, which was recorded hourly, was collected from three ground stations: NNRC.SFS, S6_R, and S6R_Z. S6_R was located approximately 150 feet to the east of the S6 sampling point, S6R_Z approximately 1.15 miles northwest of the northeastern corner of the study area, and NNRC.SFS approximately 4.15 miles northwest of G434. The three precipitation ground station data, shown separately on Figure 28, followed a similar pattern to the nitrogen but a more seasonal pattern could be seen. The addition of the

moving average trendline was not necessary to show seasonality due to the thousands of hourly recorded precipitation data points.

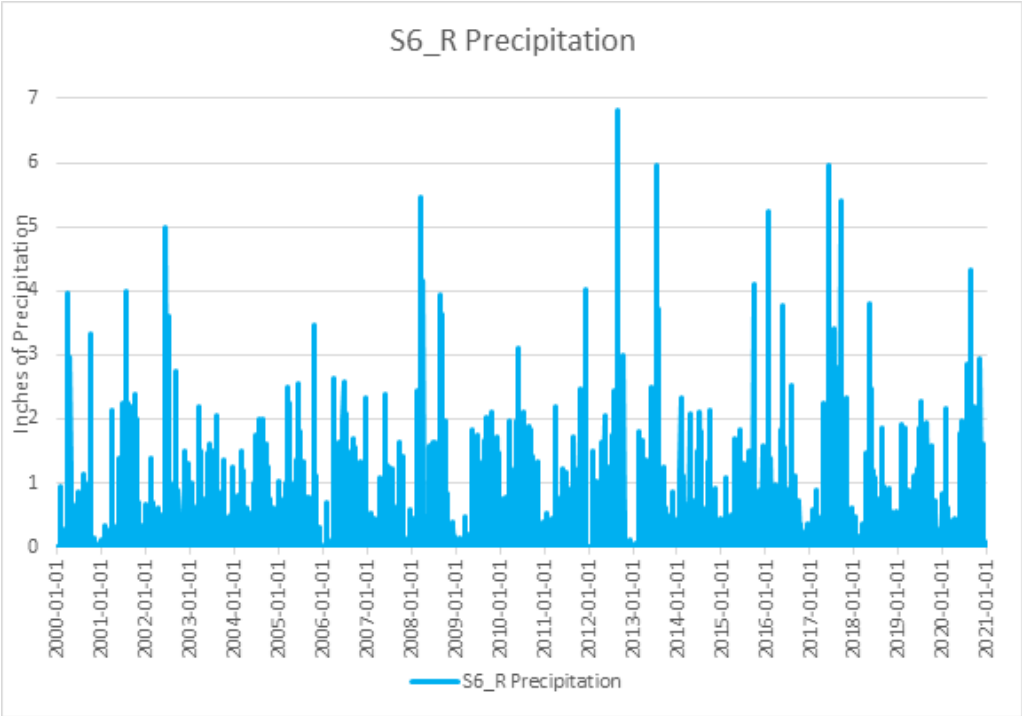

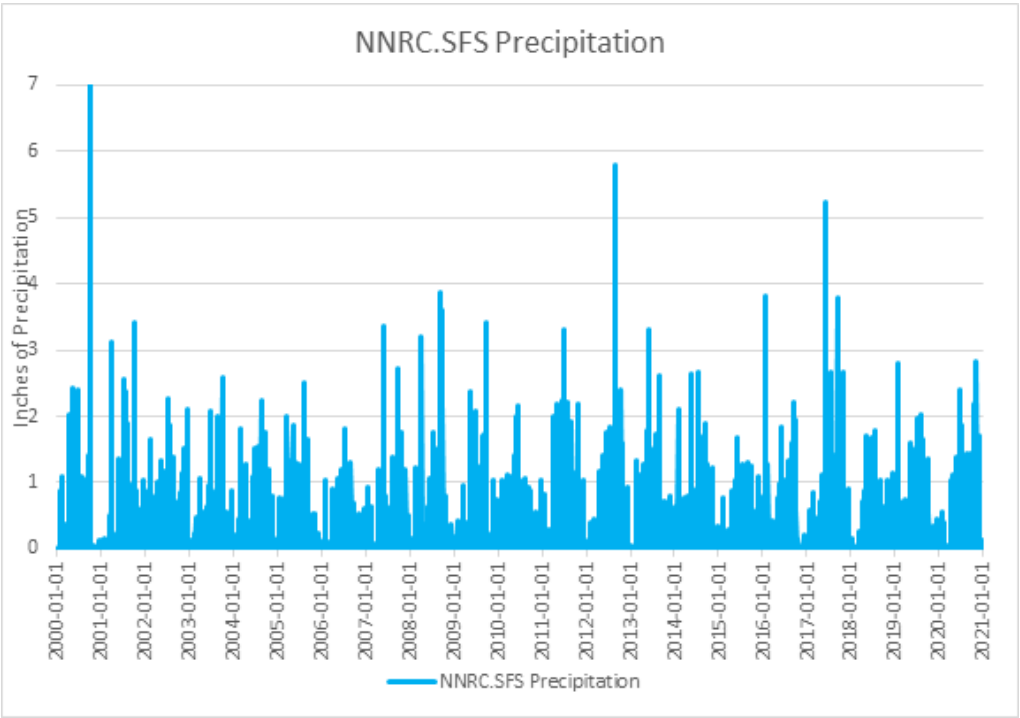

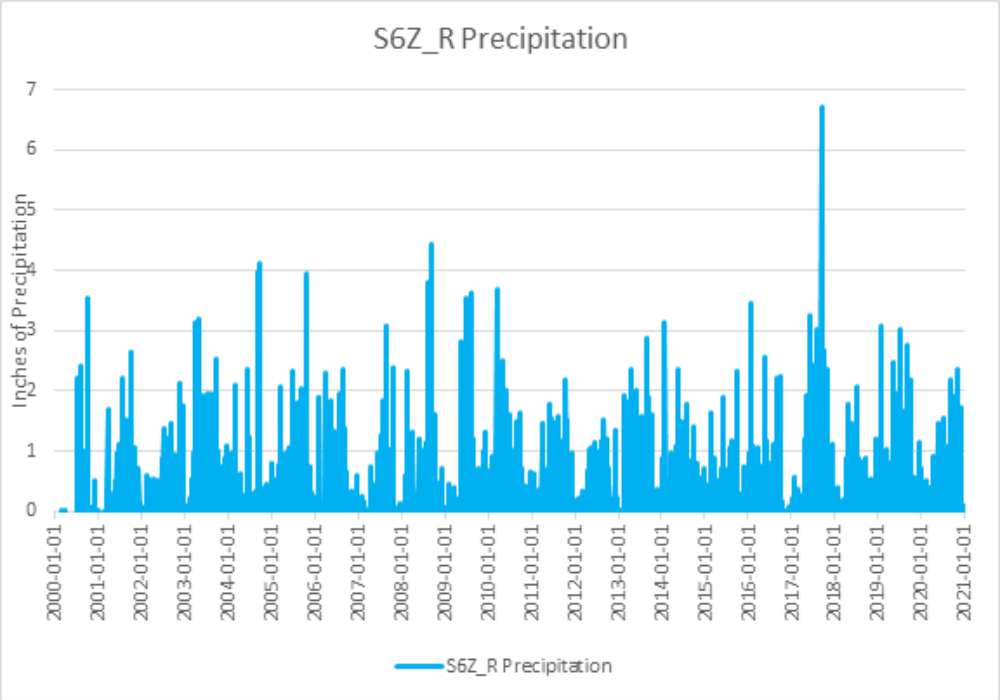

Figure 28. NNRC.SFS, S6_R, & S6Z_R precipitation graphs.

Precipitation data from January 2000 to December 2020 for the NNRC.SFS, S6_R, and S6Z_R ground stations. The precipitation data is hourly recordings.

Figure 29 juxtaposes the nitrogen and precipitation data, illustrating the density of data points. The trends of the precipitation data followed a very similar pattern, illustrating a general continuity of precipitation throughout the study area.

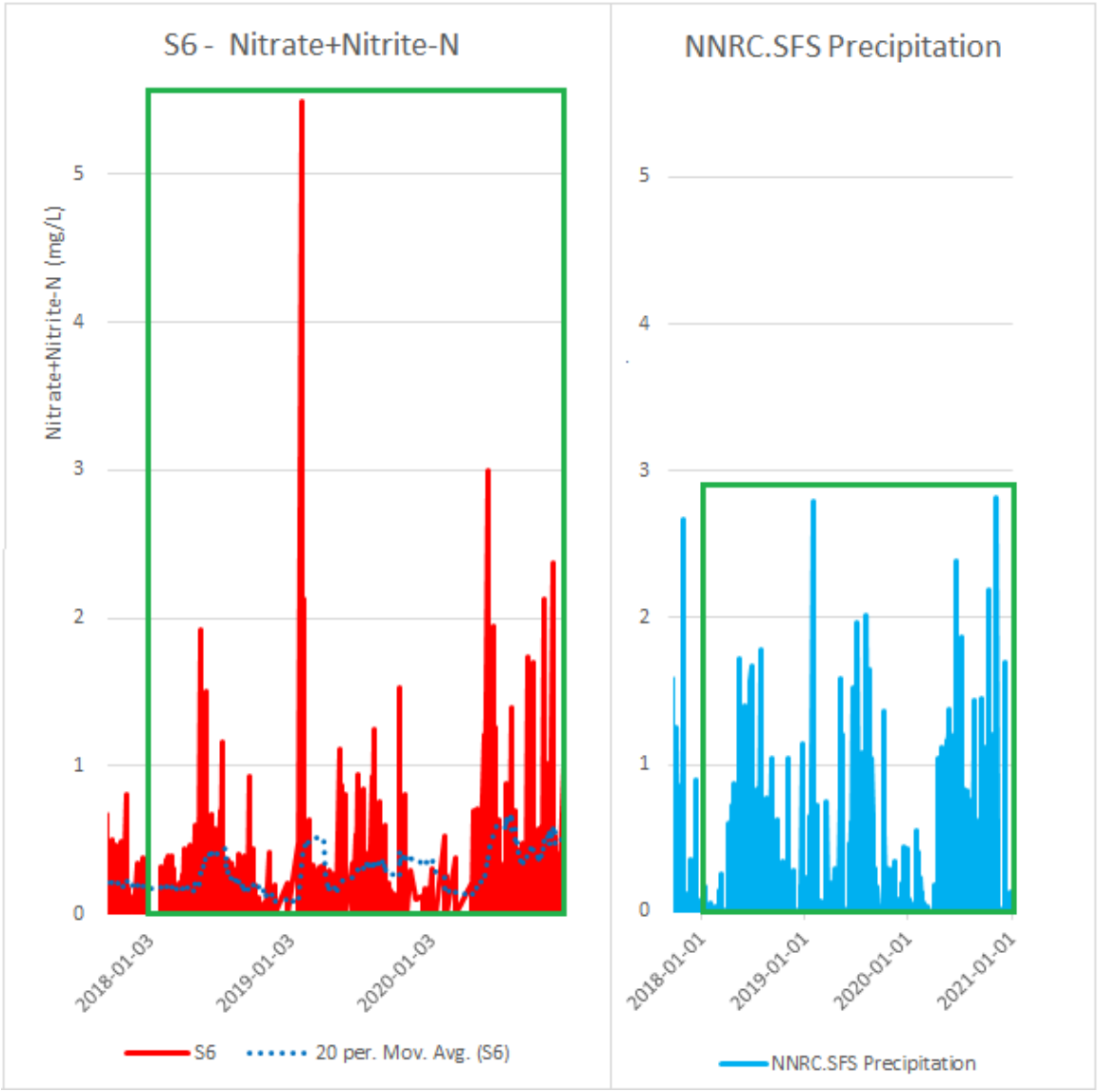

Figure 29. Juxtaposed nitrogen and precipitation graphs at S6.

Nitrogen and precipitation data from January 2018 to December 2020, delineated by the green box, for the S6 and NNRC.SFS ground stations, respectively. 267 nitrogen data points and 1,096 precipitation data points. Clearer curves can be observed in the precipitation graph.

Satellite Data

The supervised thresholding of the NDVI values were based on the visual interpretation and inspection of the NDVI values within that ground cover type; the

NDVI values for each ground cover classification was presented in Table 6. The healthy sugarcane illustrated a very high NDVI response, due to the large number of green leaves present on the plant. The burned fields showed a low NDVI response, as the green leaves and green trash had been burned away, leaving dark brown stalks and dark gray to black soil exposed.

The NBR, due to the Red and NIR bands both having positive slopes, generally followed the same pattern as the NDVI, i.e., sugarcane had high values and burned fields had low values. The ground cover types were classified by: selecting the burned ground first, due to the ease of identifying it; the healthy sugarcane fields second, done easily due to great prevalence of sugarcane throughout the study area; clouds third, the clouds were easily identified but the cloud shadows had to carefully inspected to determine if the NDVI value were actually affected; and lastly, the gap between the burned ground and healthy sugarcane, essentially defined by default. Figures 30 and 31 are photographs of typical sugarcane. As observed in the photograph, sugarcane remains clumped together and does not spread, resulting in exposed soil.

I determined the middle gap was regrowing sugarcane fields (Figure 31) from the seasonality of sugarcane harvest and by my visual inspection of various fields. Figure 31 clearly shows the exposure difference of the soil of young sugarcane versus more mature sugarcane. The LandSat data will incorporate the visible soil in the NDVI value, per pixel, due to the 30-meter special resolution. The middle gap also included atypical ground cover types, fallowed fields and cover crops. Cover crops were not prevalent in early years of the study and are only present in limited amounts by 2020. Both of the atypical ground covers did not interfere with my analysis of the study area.

However, the most important ground cover is the burned ground. This allowed me to define a numerical limit for use in the statistical analyses. The now clearly defined burned ground value range allowed for the eventual limit on the anomalous value calculations.

Figure 30. Sugarcane and peat soil photograph.

View of the typical peat soil sugarcane is grown in. The spacing between the sugarcane is approximately 3 feet. Photograph taken by the author.

Figure 31. Photographs of sugarcane fields.

View of young sugarcane (top picture). Note the soil between the rows is completely exposed. The more mature sugarcane (bottom picture) has little soil exposure. Photographs taken by the author.

Figure 32 is a cross sectional view of a sugarcane field showing a dry fallowed field underlain by limestone. Cracks and clumping of the peat layer are visible; peat breaks down when exposed to oxygen and is more easily eroded. This particular field does not show any form of erosional control to prevent soil loss during rain events. As discussed in the next section, large precipitation events appear not to be needed to cause nitrogen loss, thus soil loss. My second hypothesis posited that a change in the burning practice to a more sustainable practice could prevent this loss. It is clear from Figures 30-32 that the current sugarcane management practices are not protecting the peat. And as previously discussed, the peat shown in Figure 32 is highly flammable thus resulting is a more susceptible environment for erosion.

Figure 32. Cross sectional view of dry peat underlain by limestone.

Source: UF IFAS, Everglades Agricultural Area Soil Subsidence and Sustainability.

To address the second part of my first hypothesis, if regional differences were observed in the scale of burning each year and environmental impact, I compared the variables, NDVI, precipitation, and nitrogen from each region where ground station data were available (G328, G434, and S6) (Figure 7).

To determine the scale of burning, I utilized NDVI as a proxy for burning. The acquired LandSat data from 2018 to 2020 illustrated some trends, but were limited due to the three-year timeframe. The acquisition of data from Climate Engine expanded the analysis up to a two-decade time span. The NDVI Climate Engine mean values for the regions were nearly identical, within 4.8% of each other and standard deviations were within 6.4% of each other. I interpreted this as an indication the NDVI values for each region were similar for each region over the twenty years. By visually inspecting the fields, both in person and by satellite imagery, and observing sugarcane throughout the regions, it stands to reason sugarcane was the only crop present during the twenty years.

A comparison of the precipitation from the three ground stations would indicate if one region had unusual rainfall, which, as the driving transport mechanism for erosion, would ultimately cause a greater environmental impact, as measured by the nitrogen in the water. The precipitation mean values had a difference of only 0.02-inches and a max standard deviation of 0.05-inches. These results indicate regional variability in precipitation within the study area did not occur. Thus, erosion due to precipitation would theoretically have been very similar.

The comparison of the nitrogen data resulted in the greatest degree of variability between the three ground stations. The mean values differed by 30-68% and the standard deviations differing by 13-33%. This variability in the nitrogen is also clearly seen

graphically (Figure 24). This indicates the three regions do vary from each other in the environmental impact, but the variable to explain why these regions differ is unknown and thus a limitation of this study. These results therefore only partially support hypothesis H1b.

Time Series Results

The initial results from the 2018-2020 data showed some general trends, but due to poor quality LandSat images multiple data gaps were present in the graphs. Most data gaps overlapped between the three SPs at each region. This illustrated the seasonality of south Florida region as the data gaps were typically present during the rainy season when cloud cover affects the Landsat image quality the most. The general trend of sugarcane seasonal harvesting could be observed. A clearer sugarcane seasonality was observed in the 2000-2020 time series.

Figure 33 shows notable outliers in the data for SPs G328 and S6, indicated by Z-score anomalies; these values show conditions where likely soil loss was occurring. The driving factor of loss was precipitation, as elevated nitrogen was typically present in the spring and summer months, when precipitation is at its peak. These months were the opposite months of low NDVI values when the sugarcane is growing. Sugarcane was not a ground cover crop and the annual burning of the fields appears to perpetuate the loss of nitrogen, likely in form of soil loss. Additionally, the frequency of the nitrogen anomalies does not appear to be lessening over time. It can be assumed the soil management practices were 1) not effective on nitrogen, or 2) had not yet been implemented in this area. This result partially supports my first hypothesis, H1a, in that

an indirect correlation can be observed between the field burning and the increased nitrogen downgradient.

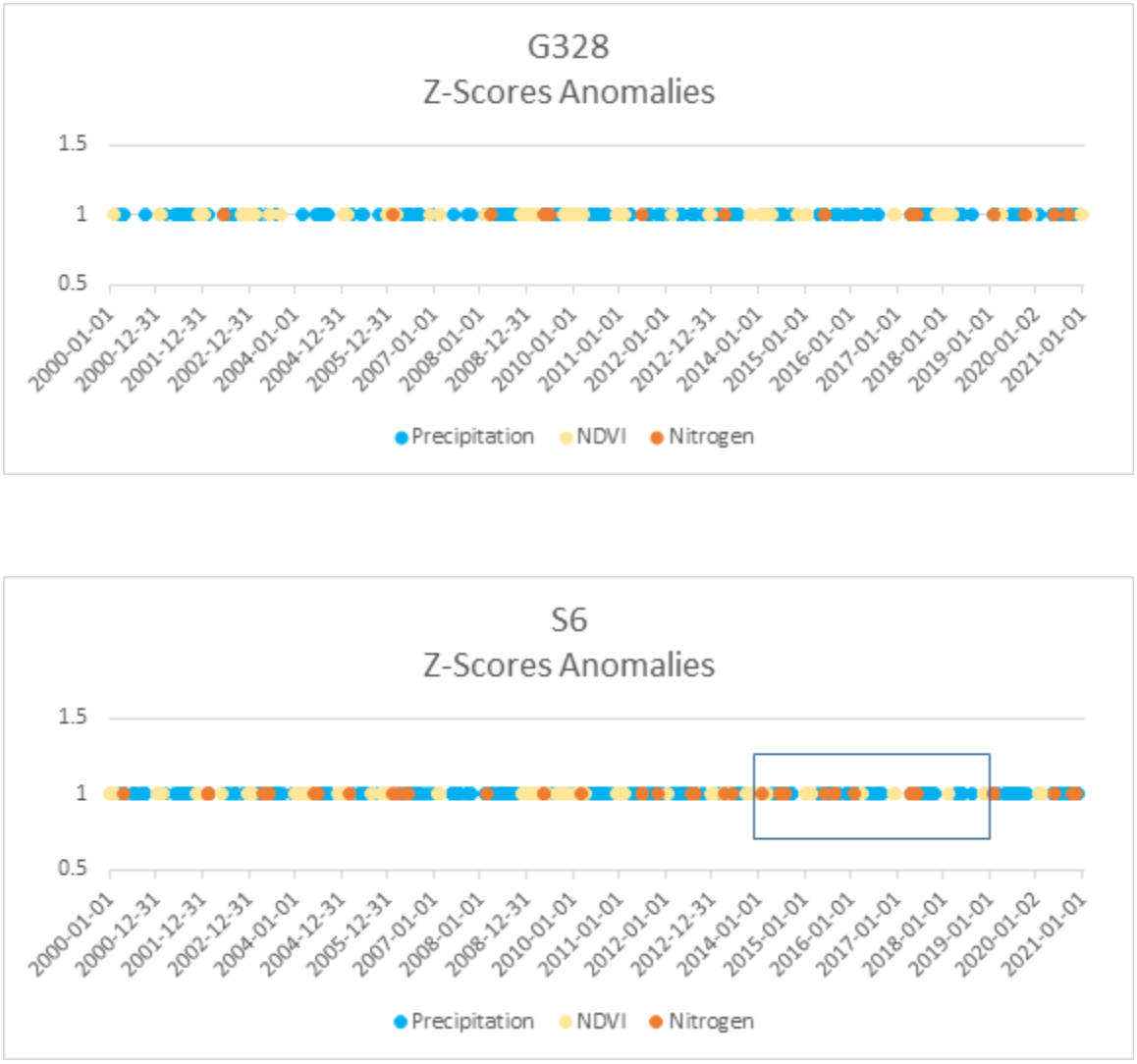

Figure 33. G328 & S6 20-year Z-score anomalies.

Twenty-year span of Z-Score anomalies for G328 and S6. The box highlights the section of time selected for Figure 34.

To allow for ease of comparison of these anomalies, a five-year timeframe was selected (Figure 34). Figure 34 compares the three ground station regions within my

study area. Precipitation was very similar, whereas NDVI, though minimally different on average, did show variability in the timing of the sugarcane growth/harvest cycle. The largest difference, however, was in nitrogen concentration.

The graphical juxtaposition of each region supports hypothesis H1b (Figure 34). The regional scale of burning, shown by proxy of low NDVI values, can be observed for each region. The greater the number of NDVI anomalies, the greater the number of nitrogen anomalies. But this appears to only hold true if enough precipitation is present as the transport mechanism of erosion.

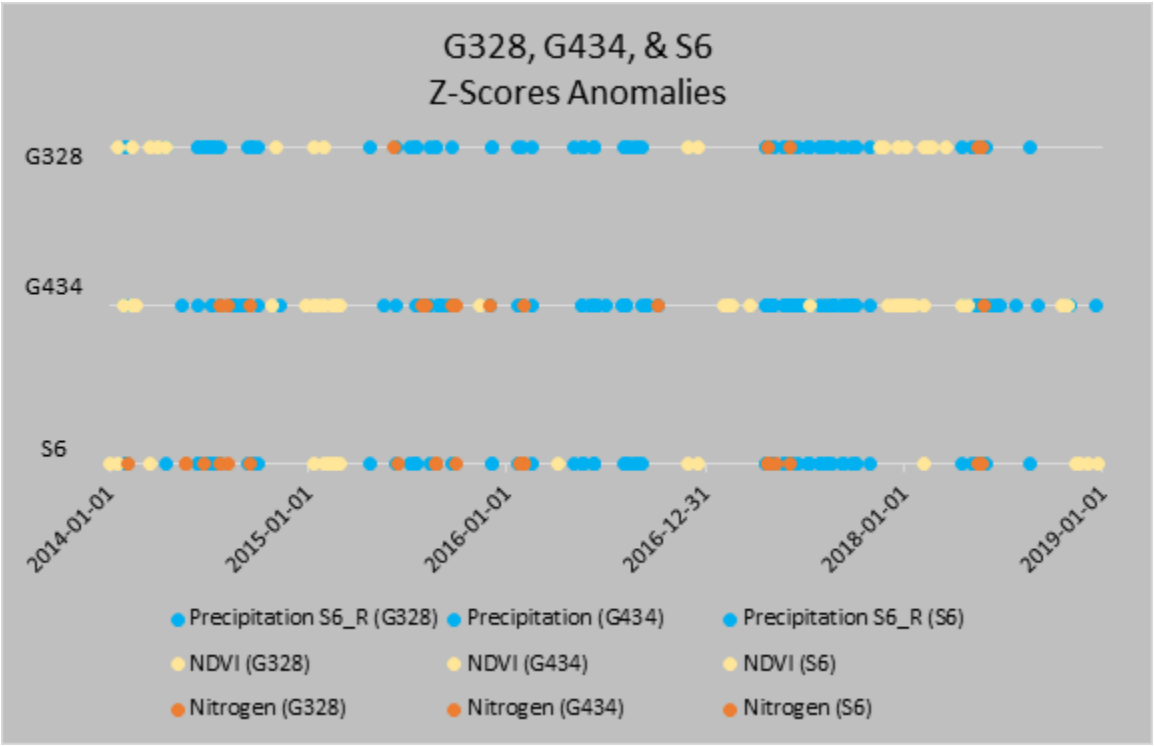

Figure 34. 5-year Z-Scores Anomalies for the G328, G434, and S6 ground stations

Graphical comparison of the three ground stations' anomalies over a five-year timespan, January 2014 through December 2018.

Cost Benefit Analyses

Three cost benefit analyses (CBA) were performed to model scenarios for potential future sustainable business practice for soil management:

1. The replacement of harvesters with a one of the newer models that increases efficiency and allows for harvesting of unburned sugarcane, leaving the green bagasse in place in the fields.
2. Harvesting the sugarcane along with the bagasse, then processing the green trash and bagasse into biochar for resale.
3. Planting Sunn Hemp as a cover crop during the fallow year to aid in soil stabilization, nutrient loss prevention, and pest control.

Options 2 and 3 both have significant potential to improve the soil and as a result reduce the environmental impact of N pollution and soil loss. All three scenarios support my H2a hypothesis that substantial environmental benefits could be realized by mitigating nitrogen by altering sugarcane farming practices.

The Total Market Value of sugar & molasses and the Net Returns Above Total Production Expenses results of the CBA for each scenario and the baseline are shown in Table 7. The ranking of the which option was the most profitable, based on category, is shown on Table 8. Option 1 was the most profitable in Total Dollar Value and Dollar Value Per Acre. This was due to harvester greatly reducing the cost of production so the value per acre increased. Option 2 was the most profitable for the Value Per Pound of Sugar, due to the added value of the biochar resale. The second most profitable for Value Per Pound of Sugar was Option 3, due to the reduction in fertilizer and pest control costs.

Table 7. Value comparisons of sustainability options for sugarcane harvesting.

		Total Dollar Value	Dollar Value Per Acre	Value Per Pound of Sugar
Baseline	Total Market Value of Sugar & Molasses	$253,674,960.00	$2,719.15	$0.21
	Net Returns Above Total Production Expenses	$87,284,583.60	$935.61	$0.071
Option 1	Total Market Value of Sugar & Molasses	$291,726,204.00	$3,127.02	$0.21
	Net Returns Above Total Production Expenses	$101,501,910.26	$1,088.00	$0.072
Option 2	Total Market Value of Sugar & Molasses	$253,674,960.00	$2,719.15	$0.21
	Net Returns Above Total Production Expenses	$93,850,357.88	$1,005.99	$0.077
Option 3	Total Market Value of Sugar & Molasses	$253,674,960.00	$2,719.15	$0.21
	Net Returns Above Total Production Expenses	$88,794,633.60	$951.79	$0.073

Comparison of the market value of sugar and molasses and the net returns above total production expense for the baseline and three sustainability options.

Table 8. Profitability ranking of the baseline and three options for sugarcane harvesting.

Profitability (most to least)		
Total Dollar Value	**Dollar Value Per Acre**	**Value Per Pound of Sugar**
Option 1	Option 1	Option 2
Option 2	Option 2	Option 3
Option 3	Option 3	Option 1
Baseline	Baseline	Baseline

Chapter IV

Discussion

These results indicated nitrogen was being introduced into the study area from a source within the study area. The very likely source was the nitrogen-rich peat. The timeseries of the ground station variables indicated that the nitrogen being introduced into the groundwater varied by region, thus supporting hypothesis H1b.

The analysis of the z-score anomalies illustrated the seasonality of the nitrogen, NDVI, and precipitation. The unexpected result was that the nitrogen anomalies typically only occurred during the rainy season and only if precipitation anomalies were present. This did support hypothesis H1a, but not perfectly. Further research could be done on the how precipitation causes the loss of nitrogen, and how this is related to the instability of the peat.

The cost benefit analyses illustrated that each of the sustainability options were financially viable; therefore, the practice of burning the sugarcane fields could cease without compromising sugarcane profitability. This supported hypothesis H2b, and CBA Options 2 and 3 supported H2a.

Research Limitations and Recommendations

Multiple challenges were encountered during each phase of this research. The initial, and perhaps the most severe, was the lack of ground station data within my study area. This limited the amount of data that could be analyzed, but fortunately multiple ground stations were present with enough data to proceed with the study. Future studies

would benefit by the addition of at least one ground station on each major canal within the EAA.

A second limitation was the low number of satellite images each year and the spatial resolution available. Due to the limitation of the LandSat satellite's orbit, daily images were not available to calculate the growth and burning of each field with more accuracy. Another limitation of relying on satellite images were the atmospheric conditions; cloud cover can cause significant interference or render an image completely useless. This was a contributing factor to extending my date range to two decades.

The incorporation of additional satellite data, either from public (such as Sentinel-2) or private sources, would greatly enhance the NDVI analyses and consequently improve the statistical comparison of variables. The additional data would also have the potential to capture pre, during, and post sugarcane field burning for a single field. This would help improve the ground cover classification of the burned ground cover class.

The three regions differed in their N pollution detections, but the variable(s) that explain this spatial variation is unknown. Further soil studies could be performed on the three regions, focusing on why they react differently. The focus on soil type, structure, biological activity, and chemistry could aid in determining whether a particular soil type is more prone to erosion within the EAA. This could then be used to develop or adjust the soil management best practice(s) to help slow or potentially prevent the loss of soil.

I encountered several challenges in constructing the CBA models. In an effort to reduce complexity and potential errors, I made multiple assumptions: that the production of sugarcane each year did not change; that the costs for various items were typical retail prices; that the unit prices would be lower due to bulk quantity price reductions; and with

the scale of sugarcane production. For instance, the machinery prices were the base prices only, but the actual cost would be higher based on the custom needs of the purchaser. However, it is unlikely the price would increase enough to severely impact the model calculations and conclusions.

The CBA models illustrated profitability in all three scenarios, but this would not scale to very small farms, given to the high capital costs of machinery. The only likely option for increasing sustainability on a small production farm would be Option 3. It would also be possible for a small farm to rent newer harvesters, but a specific CBA would need to be done to evaluate profitability.

Conclusions

I have explored multiple sources of data pertaining to a defined section within the Everglades Agricultural Area. After analyzing the data, I concluded that the practice of burning the sugarcane fields remains as a source of negative environmental impacts through nitrogen pollution, and further, by the continued loss of highly organic soil. This continued observed loss of soil within my study area presents a major sustainability problem for the sugarcane industry. If soil loss continues, the underlying limestone and quartz sand will be the soil in which the sugarcane will have to grow. The University of Florida IFAS has multiple studies on the reduced yield of sugarcane in sand and limestone soils. It is the best interest of the sugarcane farms to adjust their soil management strategies while the peat is still present.

I then presented multiple options for sugarcane companies to cease burning and yet remain profitable. I believe the sustainable options presented can be a win-win for

the environment and the sugarcane farms, resulting in a long, prosperous, sustainable, and symbiotic relationship.

References

Anderson, D., & Rosendahl, P. (2007). Development and management of land/water resources: the Everglades, agriculture, and south Florida. *Journal of the American Water Resources Association*, *34*, 235-249. https://doi.org/10.1111/j.1752-1688.1998.tb04131.x

Ball-Coelho, B., Tiessen, H., Stewart, W., Salcedo, I., & Sampaio, E. (1993). Residue management effects on sugarcane yield and soil properties in Northeastern Brazil. *Agronomy Journal*, *85*, 1004-1008. https://doi.org/10.2134/agronj1993.00021962008500050009x

Baucum, L., & Rice, R. (2009). An Overview of Florida Sugarcane. *University of Florida/IFAS EDIS SS-AGR-232*. https://doi.org/10.32473/edis-sc032-2009

Bhadha, J., Xu, N., Khatiwada, R., Swanson, S., LaBorde, C. (2020). Bagasse: A Potential Organic Soil Amendment Used in Sugarcane Production. *University of Florida/IFAS EDIS SL477*. https://edis.ifas.ufl.edu/publication/SS690

Brumbley, S., Snyman, S., Gnanasambandan, A, Joyce, P., Hermann, S., Silva, J., McQualter, R., Wang, M., Egan, B., Patterson, A., Albert, H., & Moore, P. (2009). *A Compendium of Transgenic Crop Plants: Sugar, tuber, and fiber crops* (Vol. 7). Wiley.

Climate Engine. (2022). *Research app – Climate Engine*. Retrieved from https://app.climateengine.com/climateEngine

Comstock, J., Glaz, B., Tai, P.Y.P., Edmé, S., Morris, D., & Gilbert, R. (2004). United States Department of Agriculture-Agricultural Research Service, Sugarcane Field Station at Canal Point, Florida: Past, present, and future. *International Sugar Journal*, *106*, 663-668.

Corstanje, R, Grafius, D., Zawadzka, J, Moreira Barradas, J, Vince, G, Ivanoff, D, & Pietro, K. (2016). A datamining approach to identifying spatial patterns of phosphorus forms in the Stormwater Treatment Areas in the Everglades, US. *Ecological Engineering*, *97*, 567-576.

Daroub, S., Van Horn, S., Lang, T., & Diaz, O. (2011). Best management practices and long-term water quality trends in the Everglades Agricultural Area. *Critical Review in Environmental Science and Technology*, *41*, 608-632.

Deliberto, M., & Hilbun, B. (2019). 2019 Projected Sugarcane Production Farm Costs and Returns Model. Louisiana State University Agricultural Center. Department

of Agricultural Economics & Agribusiness – Staff Report. https://www.lsuagcenter.com/articles/page1546614463631

Department of Army. U.S. Army Corps of Engineers (2018). *Integrated Feasibility Study and Draft Environmental Impact Statement*. https://usace.contentdm.oclc.org/

Franco, H., Otto, R., Faroni, C., Vitti, A., Oliveira, & E., Trivelin, P. (2011). Nitrogen in sugarcane derived from fertilizer under Brazilian field conditions. *Field Crops Research*, *121*(1), 29-41.

Heitmann, J. (1998). The beginnings of big sugar in Florida, 1920-1945. *The Florida Historical Quarterly*, 77(1), 39-61.

Jeong, C., DeRamus, A., Goodeaux, J. & Goodeaux, L. (2012). Effects of residue management on nitrogen losses in surface and sub-surface water from sugarcane fields. *Archives of Agronomy and Soil Science*, *60*, 103-118.

Julian, P., Gilhooly, A., Payne, G., & Zue, S. (2020). Chapter 3A: Water quality in the Everglades Protection Area. *2020 South Florida Environmental Report*, *1*.

Marioano, E., Leite, J., Megda, M., Torres-Dorante, L., & Trivelin, P. (2015). Influence of nitrogen form supply on soil mineral nitrogen dynamics, nitrogen uptake, and productivity of sugarcane. *Agronomy Journal*, *107*(2), 641-650.

McCray, J., Mabry, Ji, Shangning, & Ulloa, Modesto. (2017). Influence of compost/sludge application on sugarcane yield and nitrogen requirement on a sand soil. *Journal of Plant Nutrition*, *40*(15), 2156-2167.

McCray, J., Morgan K/. & Baucum L. (2016). Nitrogen Fertilizer Recommendations for Sugarcane Production for Sugar on Florida Sand Soils. *University of Florida/IFAS EDIS SS-AGR-401*. https://edis.ifas.ufl.edu/publication/SC101

McCray, J., Sandhu, R., Rice, R., & Odero, D. (2019). Nutrient requirements for sugarcane production on Florida muck soils. *University of Florida/IFAS EDIS SS-AGR-226*. https://edis.ifas.ufl.edu/publication/SC026

Muwamba, A. (2012). Nitrogen and phosphorus movement in sandy soils of south Florida used for sugarcane production with elevated water table. *Dissertation Abstracts International*, *74*, 09(B), 252.

Petuch, E., & Roberts, C. (2007). *The geology of the Everglades and adjacent areas*. CRC Press.

Picoli, M., Araújo, C., Machado, P., Gerber, D., Garbellini, D., Scarpare, F., Vale, C., Ruiz, S., Hernandes, T., Dourado, A., & Rocha, J. (2019). Sugarcane drought detection through spectral indices derived modeling by remote-sensing techniques. *Modeling Earth Systems and Environment*, *5*(4), 1679-1688.

QGIS Project. (2021). *QGIS* (Version 3.16). QGIS Project. https://www.qgis.org/en/site

Rice, R., Gilbert, R., & Daroub, S. (2005). Application of the soil taxonomy key to the organic soils of the Everglades Agricultural Area. *University of Florida/IFAS EDIS SS-AGR-246*.

Rott, P. (2017). *Achieving sustainable cultivation of sugarcane Volume 1*. Burleigh Dodds Science Publishing. https://doi.org/10.4324/9781351114356

Rott, P., Odero, D., Beuzelin, J., Raid, R., VanWeelden, M., Swanson, S., & Mossler, M. (2018). Florida Crop/Pest Profile: Sugarcane. *University of Florida/IFAS EDIS PI-171*. https://edis.ifas.ufl.edu/publication/PI207

Ruschel, A. Puppin, & Vose, P.B. (1982). Nitrogen cycling in sugarcane. *Plant and Soil*, *67*(1/3), 139-146.

Sandhu, H., Gilbert, R., Shine, J., Rice, R., & Odero, D. (2016). Maturity Curves and Harvest Schedule Recommendations for CP Sugarcane Varieties. *University of Florida/IFAS EDIS SS-AGR-221*. https://edis.ifas.ufl.edu/publication/SC069

Sandhu, D., Singh, A., Fan, N., Wang, D., & Duranceau, S. (2016). Hydro-geomorphic response of Everglades to changing climate and anthropogenic activities. *Journal of Hydrology*, *543*, 861-872.

Seeteram, N., Engel, V., & Mozumder, P. (2018). Implications of a valuation study for ecological and social indicators associated with Everglades restoration. *The Science of the Total Environment*, *627*, 792-801.

Schmitz, A., & Zhang, F. (2019). The dynamics of sugarcane and sugar yields in Florida: 1950-2018. *Crop Science*, *59*(5), 1880-1886.

United States Geological Survey. (2021). LandSat missions. Retrieved from https: www.usgs.gov/core-science-systems/nli/landsat

United States Geological Survey. (2022). EarthExplorer. Retrieved from https://earthexplorer.usgs.gov/

Udeigwe, T., Wang, J., Viator, H., & Gaston, L. (2010). Surface water quality as affected by sugarcane residue management techniques. *Water, Air, and Soil Pollution*, *208*(1-4), 119-128.

Velini, E., Trindade, M., Barberis, L., & Duke, S. (2010) Growth regulation and other secondary effects of herbicides. *Weed Science*, *58*(3), 351-354.

Vera, J., Valeiro, A., Posse, G., & Acreche, M. (2017). To burn or not to burn: the question of straw burning and nitrogen fertilization effect on nitrous oxide emissions in sugarcane. *Science of the Total Environment*, *587-588*, 399-406.

Villareal, M. K. (2020) Remote sensing techniques for classification and mapping of sugarcane growth. *Engineering, Technology, & Applied Science Research*, *10*(4), 6041-6046.

Willis, J., & Hester, M. (2015). Evaluating postharvest sugarcane residue amendment and broadcast fertilizer application as techniques to enhance dune grass establishment and expansion. *Ecological Restoration*, *33*(2), 190-196.

Wright, A., & Hanlon, E. (2019). Organic matter and soil structure in the Everglades Agricultural Area. *University of Florida/IFAS EDIS SL301*. https://edis.ifas.ufl.edu/publication/SS514

Zhang, C. (2020). Multispectral Remote sensing Applications. *Multi-sensor system applications in the Everglades ecosystem*. CRC Press.